FLT3 signaling inhibition abrogates opioid tolerance and hyperalgesia while preserving analgesia

Antoine Jouvenel, Adrien Tassou, Maxime Thouaye, Jérôme Ruel, Myriam Antri, Aurore Giraudin, Sylvie Mallié, Chamroeum Sar, Lucie Diouloufet, Corinne Sonrier, et al.

nature communications

Article

https://doi.org/10.1038/s41467-024-54054-y

FLT3 signaling inhibition abrogates opioid tolerance and hyperalgesia while preserving analgesia

Received: 6 December 2023

Accepted: 30 October 2024

Published online: 07 November 2024

Check for updates

Antoine Jouvenel[1,2,7], Adrien Tassou[1,2,7], Maxime Thouaye[1,2,7], Jérôme Ruel[3], Myriam Antri[4], Jean-Philippe Leyris[5], Aurore Giraudin[4], Sylvie Mallié[2], Chamroeum Sar[1,2], Lucie Diouloufet[2,5], Corinne Sonrier[2,5], François Daubeuf[6], Juliette Bertin[2,5], Stacy Alves[1,2], Stéphanie Ventéo[1,2], Nelly Frossard[6], Patrick Carroll[1,2], Ilana Mechaly[1,2], Didier Rognan[6], Pierre Sokoloff[5], Radhouane Dallel[4], Patrick Delmas[3], Jean Valmier[1,2] ✉ & Cyril Rivat[1,2] ✉

Navigating the duality of opioids' potent analgesia and side effects, including tolerance and hyperalgesia, is a significant challenge in chronic pain management, often prompting hazardous dose escalation to maintain analgesic effects. The peripheral mu-opioid receptor (MOR) is known to mediate these contradictory effects. Here, we show that the fms-like tyrosine kinase receptor 3 (FLT3) in peripheral somatosensory neurons drives morphine tolerance and hyperalgesia in a male rodent model. We found that chronic morphine treatment increases FLT3 and MOR co-expression, and that inhibiting FLT3 represses MOR-induced hyperactivation of the cyclic adenosine monophosphate (cAMP) signaling pathway, mitigating maladaptive excitatory processes engaged after chronic morphine treatment. Furthermore, in postsurgical or inflammatory models of chronic pain, co-administering morphine with a FLT3-specific inhibitor not only prevents or suppresses tolerance and hyperalgesia but also potentiates the analgesic efficacy of morphine, without aggravating other morphine-induced adverse effects. Our findings suggest that pairing morphine with FLT3 inhibitors could become a promising avenue for chronic pain management to safely harness the power of opioids, without the risk of dose escalation. By enhancing morphine analgesic potency through FLT3 inhibition, this approach could minimize opioid dosage, thereby curtailing the risk of addiction and other opioid-related side effects.

While opioid analgesics stand unrivaled in managing severe pain, particularly in acute and cancer-related scenarios, their long-term employment in treating other chronic pain disorders has encountered escalating scrutiny. Long-term opioid therapies are inadequate due to their declining long-term efficacy[1] linked to the onset of analgesic tolerance leading to dose escalation, paradoxical hyperalgesia[2–4], and other harmful side effects, such as addiction and life-threatening respiratory depression[5]. Current pharmaceutical strategies fall short of

[1]Université de Montpellier, Montpellier, France. [2]Inserm U–1298, Institut des Neurosciences de Montpellier, Montpellier, France. [3]Centre de Recherche en CardioVasculaire et Nutrition, Aix-Marseille Université - INSERM 1263 -INRAE 1260, Marseille, France. [4]NeuroDol INSERM 1107, Clermont-Ferrand, France. [5]Biodol Therapeutics, 165 rue Denis Papin, Montarnaud 34570, France. [6]Laboratoire d'Innovation Thérapeutique, UMR7200 CNRS/Université de Strasbourg, 67400 Illkirch, France. [7]These authors contributed equally: Antoine Jouvenel, Adrien Tassou, Maxime Thouaye. ✉e-mail: jean.valmier@umontpellier.fr; cyril.rivat@umontpellier.fr

resolving the maladaptive processes that precipitate the progressive decline in opioid effectiveness, underscoring the urgent need for new therapeutics that can alleviate opioid-associated tolerance and hyperalgesia, thereby enhancing chronic opioid efficacy.

The G-protein-coupled mu-opioid receptor (MORs) is acknowledged as the primary contributor of opioid analgesia and side-effects[2]. Although MOR is expressed throughout pain neural circuits in a variety of nervous system regions, dysregulation of MOR function in dorsal root ganglion (DRG) neurons appears to be one of the key molecular events that initiates chronic opioid-induced pathological plasticity within the central pain circuits, thereby facilitating the development of chronic opioid-induced tolerance (OIT) and hyperalgesia (OIH)[6–8]. For example, mice lacking MOR expression in *Trpv1*+ nociceptors do not develop OIT and OIH after chronic morphine treatment while antinociception is conserved[7]. These data indicate that the mechanisms underlying OIT and OIH can be dissociated from the ones underlying analgesia, though they remain largely unexplored.

OIH and OIT represent adaptive processes in response to either acute or chronic opioid exposure that result from complex alterations of MOR at the molecular level as well as at the cellular and circuit levels, in both the peripheral and central nervous systems[7]. The mechanisms supporting OIT and OIH are tightly coupled. Indeed, the prevention of OIH can reverse OIT and restore opioid analgesic effects[2,9,10]. At the MOR level, signaling pathways (e.g. Gi/o and β-arrestin) engaged by MOR activation may cause desensitization[11,12], internalization, phosphorylation and heterodimerization[13,14] that can all participate in the development of both OIT and OIH. In addition, the long-term silencing of neurons originating from the overactivation of MOR has been suggested to be compensated by opposing mechanisms leading to increased synaptic excitability via increased excitatory neuropeptide expression[15–18] and long-term potentiation (LTP) in the spinal cord, two mechanisms also involved in OIT and OIH[7,19]. In the DRG, chronic morphine treatment can initiate the cyclic adenosine 3′, 5′-monophosphate (cAMP)/protein kinase A (PKA) pathway known as "cAMP superactivation" by activating MOR[20–22], increasing the proportions and the activity of different excitatory channels (e.g., Ca^{2+}, TRPV1 channels) and inducing pro-nociceptive glutamate and peptide release, e.g., substance P, calcitonin gene-related peptide (CGRP). This then results in primary afferent hyperexcitability, increased central neurotransmission, and dorsal spinal cord (DSC) pain sensitization[2,3,5,23,24]. Despite the consensus that cAMP/PKA signaling contributes to cellular adaptations associated with chronic opioid leading to OIT and OIH, the molecular actors and partners of MOR underlying these effects are yet to be identified.

Neuronal adaptations that are implicated in OIT and OIH share similar molecular mechanisms with those underpinning the development of peripheral neuropathic pain (PNP)[25–28]. We have previously found that PNP initiation and maintenance are dependent on fms-like tyrosine kinase receptor 3 (FLT3) activation in primary sensory neurons[29]. Activation of FLT3 by its ligand FL induces excitatory responses that result in enduring hyperexcitability of DRG neurons, central sensitization of the DSC, and heightened pain sensitivity similar to chronic opioid mechanisms mentioned above. Conversely, specific genetic or pharmacological FLT3 inhibition reverses established PNP symptoms and their molecular and cellular counterparts - inhibition of TRPV1 channel over-activation and decrease in neuropeptide upregulation. Given the ability of MOR in the DRG to functionally interact with other molecular partners such as receptor tyrosine kinases (RTK)[30–32], and the parallels between chronic morphine-induced MOR-dependent and PNP-induced FLT3-dependent pain sensitization, we were prompted to examine a potential contribution of FLT3 to MOR-dependent adaptive changes related to OIT and OIH.

Our study evidenced that FLT3 becomes activated in DRG nociceptors during long-term morphine exposure. This activation is a critical process that controls the peripheral mechanisms underlying morphine-induced adaptive changes within nociceptive neural circuits resulting in OIT and OIH. Therefore, FLT3 expressed in primary afferent sensory neurons appears to drive the initiation of adverse counter-adaptive mechanisms to morphine exposure, allowing the onset of OIT and OIH. Our data support the development of therapeutic strategies for disrupting FLT3 signaling to maintain adequate morphine pain relief, while limiting dose escalation and subsequent detrimental morphine-induced clinical side effects.

Results

FLT3 mediates morphine-induced hyperalgesia through the activation of pro-nociceptive pathways

Firstly, considering the role of DRG neurons in the control of MOR- and FLT3-dependent hyperalgesia[7,29], we compared the cellular localization of MOR and FLT3 in the lumbar DRG neurons of control mice treated with saline with those receiving repeated morphine treatment (Chronic morphine: 10 mg/kg, subcutaneous injections, twice daily for 4 days). To assess the co-expression of MOR and *Flt3*, we used the MOR-mCherry mouse line combined with in situ hybridization of *Flt3* mRNA. In control mice, we observed that 35 ± 1.6% and 25.5 ± 2.3% of DRG neurons were MOR- and *Flt3*-positive (MOR+ and *Flt3*+), respectively (Fig. 1a, b). A subset of 13 ± 1.6% of MOR+ neurons were also *Flt3*+ and 18.7 ± 3.6% of *Flt3*+ neurons expressed MOR (Fig. 1b). Strikingly, following chronic morphine exposure, the subset of *Flt3*+ neurons expressing MOR significantly increased, doubling to 34.9 ± 2.3% compared to control conditions (Fig. 1a, b) while the overall proportion of MOR+ and *Flt3*+ neurons remained relatively stable (41.6 ± 1.6% and 21 ± 1.8%, respectively). In conjunction with these results, we investigated in vivo a potential role of FLT3 on the development of OIH, using a global *Flt3*-knockout mouse model. Chronic morphine led to a gradual decrease of the mechanical pain threshold, indicating OIH, in both male and female $Flt3^{WT}$ littermate mice (Fig. 1c, S1). However, $Flt3^{KO}$ littermates of both genders failed to develop OIH (Fig. 1c, S1), signifying that FLT3 is necessary for the establishment of OIH.

To gain insights into how and where FLT3 is involved in OIH mechanisms, we evaluated the effects of FLT3 in DRG neurons on morphine-induced overactivation of cAMP, a canonical and critical second messenger of MOR for inducing OIH[20,21,33]. Initially, we observed that PKI 14-22, an inhibitor of the protein kinase A[33] which is a primary effector of the adenylyl cyclase (AC)/cAMP pathway, prevented OIH in mice when injected intrathecally (Fig. 1d). This observation underscores the role of the cAMP signaling pathway in the adaptive changes elicited by chronic morphine in vivo. Subsequently, we found that cAMP levels were elevated in DRG collected from $Flt3^{WT}$ animals treated with chronic morphine, but not from $Flt3^{KO}$ mice, when compared to $Flt3^{WT}$ animals treated with saline (Fig. 1e, S2a). Finally, we conducted primary cell culture of adult DRG neurons and evaluated the effects of chronic (Fig. 1f, S2b) or acute (Fig. S3a) morphine on forskolin-induced cAMP accumulation. As previously reported[20–22], acute morphine inhibited forskolin-induced increase of cAMP levels in DRG primary cultures from $Flt3^{WT}$ mice (Fig. S2a). This process relies on MOR activation, as shown by the blockade of morphine-induced inhibition of cAMP accumulation by the MOR-selective antagonist CTAP. Interestingly, the inhibitory effect of morphine on forskolin-induced cAMP accumulation was totally absent in cultured DRG neurons from $Flt3^{WT}$ animals that were chronically exposed to morphine (exposure to 10 μM for 4–7 days) (Fig. 1f). By contrast, the morphine inhibitory effect was maintained in DRG neurons cultured from $Flt3^{KO}$ mice (Fig. 1f). Of note, the non-normalized data indicated a difference between $Flt3^{KO}$ and $Flt3^{WT}$ DRG neurons in cAMP baseline conditions (Fig. S2b). This may be due to a negative modulation of FLT3 signaling pathways on cAMP accumulation by cross-talk mechanisms as previously shown for neurotrophins[34] or a compensatory mechanism in the constitutive $Flt3^{KO}$ mouse. This result was unlikely due to a

https://doi.org/10.1038/s41467-024-54054-y

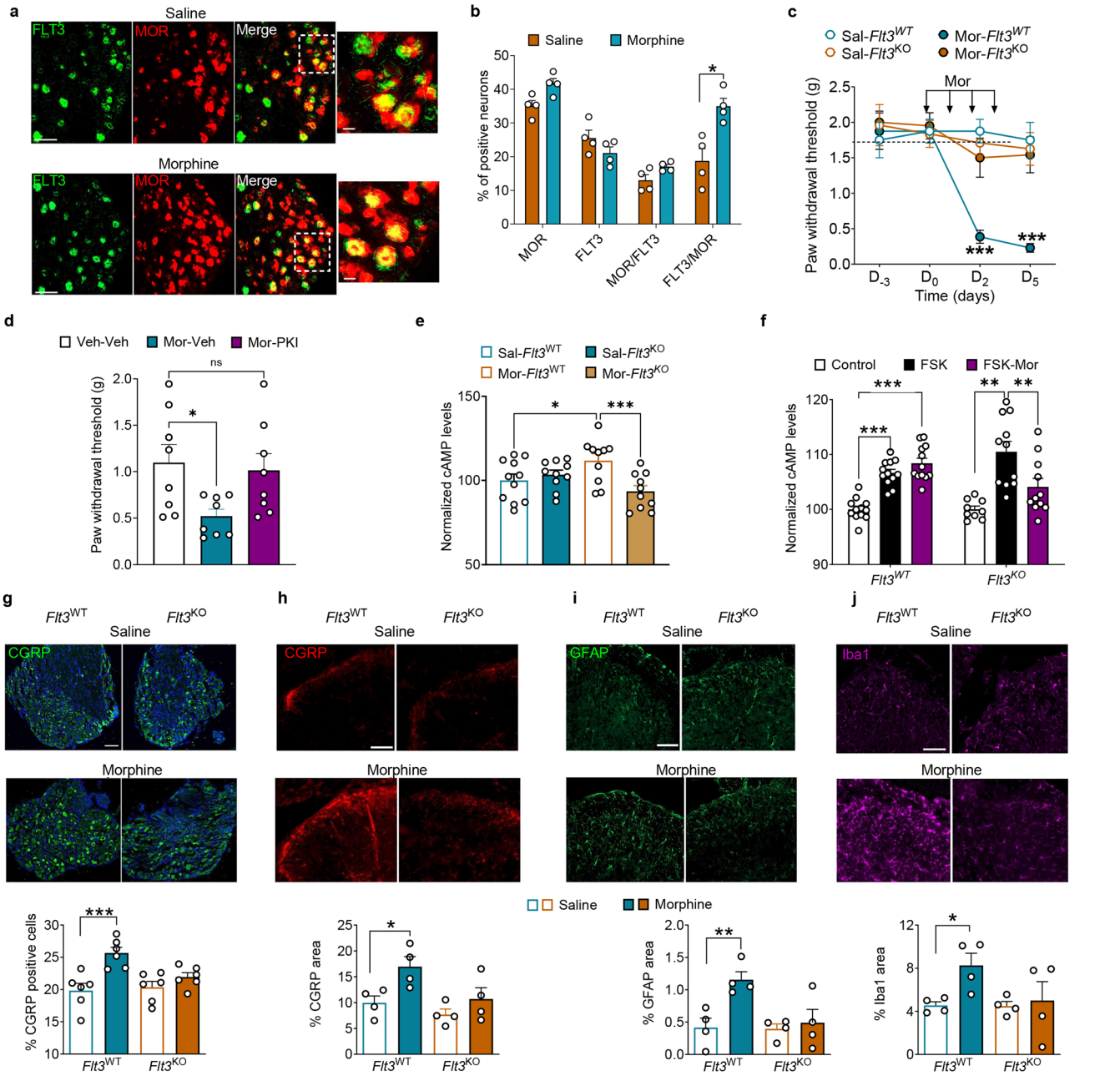

Fig. 1 | *Flt3* and MOR colocalization in mouse sensory neurons is enhanced by chronic morphine and *Flt3* invalidation blocks OIH and associated signaling and biochemical changes. a In situ hybridization of *Flt3* mRNA in DRG neurons from MOR-mCherry mice showing the colocalization of MOR and FLT3 in control mice (top) and mice repeatedly treated with morphine (bottom). Bars = 100 μm for the main pictures and 20 μm for the magnification. **b** Quantification of the images shown in (**a**) as number of positive neurons. MOR and FLT3 are the percentage of MOR+ and FLT3+ neurons respectively, among all DRG neurons. MOR/FLT3 and FLT3/MOR are the percentages of MOR+ neurons that are also FLT3+ and FLT3+ neurons that are also MOR + , respectively ($n = 4$ mice/group; $p = 0.0286$). **c** Mechanical pain sensitivity of $Flt3^{WT}$ or $Flt3^{KO}$ mice ($n = 6$) assessed by von Frey after chronic saline or morphine treatment ($p < 0.0001$). **d** Mechanical pain sensitivity of $FLT3^{WT}$ mice ($n = 8$; $p = 0.0334$) assessed by von Frey test two days after starting chronic morphine with or without PKI (5 μg i.t.). **e** cAMP dosage in DRGs from $Flt3^{WT}$ or $Flt3^{KO}$ mice treated with saline or morphine ($n = 10$ or 11; $p = 0.0234$ and $p = 0.0010$). **f** Basal cAMP level (Control), or cAMP responses to forskolin in primary cultures of DRG neurons from $Flt3^{WT}$ ($n = 4$) or $Flt3^{KO}$ ($n = 3$) mice treated with morphine. **g**–**j** Top**:** CGRP-immunoreactivity in DRG neurons ($p = 0.0004$) and CGRP-, GFAP- and Iba1-immunoreactivities, respectively, in DHSC from $Flt3^{WT}$and $Flt3^{KO}$ mice ($n = 6$) after chronic saline or morphine treatment ($p = 0.025$; $p = 0.0074$; $p = 0.0277$; respectively). Bottom: quantification of images shown in (**g**–**j**). Results are mean ± SEM of data collected from 4–6 animals. FSK, forskolin; Mor, morphine; Sal, saline. $^{*}P < 0.05$, $^{**}P < 0.01$, $^{***}P < 0.001$. Statistical analyses included two-sided Mann-Whitney test (**b**), two-way repeated ANOVA followed by adjusted Bonferroni's test for multiple comparisons (**c**, **g**–**j**), one-way ANOVA followed by uncorrected Fisher's LSD (**d**) and mixed-effect model (REML) test followed by Šidák's test for multiple comparisons (**e**). Source data are provided as a Source Data file.

difference in the expression of MOR receptors in the DRG, as no difference was found between $Flt3^{WT}$ and $Flt3^{KO}$ animals (Fig. S3b). These observations indicate that FLT3 is involved in cAMP-dependent pronociceptive changes produced by chronic morphine.

Chronic morphine treatment induces several biochemical changes, with an increase of CGRP in DRG neurons and a glial activation in the DSC being among the key alterations. These changes result in hyperexcitability of sensory nerve fibers and heighten central

neurotransmission[2,3,15,24]. Given this context, we sought to investigate FLT3's implication further by studying how *Flt3* deletion impacts these chronic morphine-induced pronociceptive phenotypes. We observed an increase in CGRP immunostaining in both DRG neurons (Fig. 1g) and their DSC projections (Fig. 1h) in $Flt3^{WT}$ mice following chronic morphine administration. This increase was absent in $Flt3^{KO}$ mice. Furthermore, glial changes as evidenced by a rise in the expression of glial fibrillary acidic protein (GFAP) in astrocytes and ionized calcium-binding adapter molecule 1 (IBA1) in microglia, were also FLT3-dependent, as these changes were substantially weaker in $Flt3^{KO}$ mice (Fig. 1i, j). Hence, our data show that biochemical changes observed after a chronic morphine treatment are dependent on FLT3, at both DRG and DSC levels.

Morphine induced-hyperexcitability is a FLT3-dependent neuronal mechanism

Next, we sought to determine whether FLT3 also regulates opiate-induced hyperexcitability of DRG neurons as typically observed in OIH and OIT. Using live microscopy coupled with intracellular Ca^{2+} ($[Ca^{2+}]_i$) imaging on primary cultures of adult mouse DRG neurons, we first examined MOR-induced ($[Ca^{2+}]_i$) changes in saline and chronic morphine conditions. Under control conditions, DAMGO (10 μM), a MOR-selective agonist that reduces neuronal excitability by inhibiting voltage-activated Ca^{2+} channels in sensory neurons[35], significantly decreased ($[Ca^{2+}]_i$) transients induced by high K^+ concentration (HiK^+) application in DRG neurons from both $Flt3^{WT}$ and $Flt3^{KO}$ mice (Fig. 2a, b). In contrast, following chronic morphine exposure (10 μM twice a day for 4 days before $[Ca^{2+}]_i$ experiments), data analysis show that application of DAMGO increased HiK^+-induced $[Ca^{2+}]_I$ transients in $Flt3^{WT}$ DRG neurons (Fig. 2a, b), confirming the excitatory effects of repeated MOR stimulation[35]. Intriguingly, the DAMGO excitatory effect was absent in neurons cultured from $Flt3^{KO}$ mice after chronic morphine treatment (Fig. 2a, b), suggesting that *Flt3* deletion can hinder the development of morphine-induced DRG neuronal hyperexcitability. In addition, analysis of non-normalized $[Ca^{2+}]$i peak transient amplitudes indicates that, under chronic morphine exposure, HiK^+-induced $[Ca^{2+}]_i$ transients was reduced in comparison with saline condition in $Flt3^{WT}$ DRG neurons (Fig. S4a, b). These results are in accordance with previous ones showing a L-type channel Ca(v)1.3 downregulation[36] and a K^+ channel Kv1.5 protein[37] upregulation under chronic morphine exposure. Such reduction was not present in $Flt3^{KO}$ DRG neurons (Fig. S4b). We also investigated the effects of the FLT3-specific negative allosteric modulator, BDT001, known to inhibit FL-induced FLT3 phosphorylation and abrogate nerve injury–induced neuropathic pain[29]. Similar to *Flt3* genetic deletion, FLT3 pharmacological blockade by BDT001 (1 μM), reversed the HiK^+-induced ($[Ca^{2+}]_i$) transient potentiation induced by DAMGO in chronic morphine-treated DRG neurons (Fig. S5a, b).

By recording single nerve fiber electrical activity using the ex-vivo glabrous skin-saphenous-nerve preparation (Fig. 2c), we observed that aberrant post-discharge activity was common in sensory fibers from morphine-treated $Flt3^{WT}$ mice after skin mechanical stimulation but was minimal or absent in fibers from chronic morphine-treated $Flt3^{KO}$ mice (Fig. 2d). In chronic morphine-treated $Flt3^{WT}$ mice, C-type sensory fibers continued to respond well beyond the cessation of the mechanical stimulus. This led to a significant 85% rise in the average firing activity of mechano-sensory fibers following the mechanical stimulation compared to the period preceding it (Fig. 2e). No post-discharges were seen in C-type sensory fibers after skin mechanical stimulation in $Flt3^{WT}$ or $Flt3^{KO}$ mice injected with saline solution instead of morphine (Fig. S6a, b; mean change in basal activity: −2.5 ± 0.5 and −1.8 ± 0.25%, respectively). Increased activity was predominantly seen in high threshold C-type mechanoreceptors (Tonic HTMRs) (+106 ± 21.8%) and low-threshold C-type slowly-adapting mechanoreceptors (SA LTMRs) (+62 ± 8%) (Fig. 2e, S6c). No post-discharges were observed in SA LTMR fibers from chronic morphine-treated $Flt3^{KO}$ mice after mechanical stimulation (Fig. 2e, S6d). Contrastingly, low-threshold rapidly-adapting mechanoreceptors (RA LTMRs) displayed no aberrant post-discharges after chronic morphine treatment in both WT and $Flt3^{KO}$ mice (Fig. 2e, S6e, d). Similarly, BDT001 (5 mg/kg), administered in vivo 90 min before each morphine administration, also abolished morphine induced-aberrant post-discharges of both HTMRs and SA LTMRs (Fig. S5c). To evaluate the effect of FLT3 silencing on excitatory properties of chronic morphine at the level of DRG central terminal synapses in the DSC, we recorded evoked-excitatory postsynaptic currents (eEPSCs) in lamina I and II outer (IIo) neurons, in response to primary afferent electrical stimulation (Fig. 2f). The recording data were obtained in unidentified post-synaptic neurons of lamina I and IIo. Chronic morphine treatment in $Flt3^{WT}$ mice significantly increased the peak amplitude of eEPSCs compared to chronic saline-treated $Flt3^{WT}$ mice (Fig. 2g, h). This morphine effect on eEPSC amplitude was not observed in $Flt3^{KO}$ mice. Altogether, our data suggest that FLT3 plays a pivotal role in promoting morphine-induced hyperexcitability across DRG fibers from peripheral to central synapses.

FLT3 inhibition in DRG neurons prevents the development of OIT and OIH

Since OIH and OIT are supported by peripheral mechanisms, we further hypothesized that FLT3 in the DRG could mediate these opioids adverse effects. Using a *Flt3*-targeted shRNA delivered via an intrathecally-injected AAV9 virus (Fig. 3a–c), we investigated whether specific FLT3 disruption in the DRG, such as the downregulation of its expression at the neuron level, would impact the development of OIT and OIH of either mice or rats. The delivery of *Flt3*-shRNA AAV9 virus reduced FLT3 expression in the DRG[29] and blocked FL-induced mechanical pain hypersensitivity, without affecting motor function in rats (Fig. S7a, c). We observed that in chronic morphine-treated rats receiving a single injection of AAV9 *Flt3*-shRNA, OIT (Fig. 3b) and OIH - mechanical pain hypersensitivity (Fig. 3c) and mechanical allodynia (Fig. S7b) - were entirely abrogated. Conversely, OIH and OIT were observed in rats receiving the control AAV9 non-targeted shRNA. Finally, the stimulation of FLT3 by intrathecal injection of the FLT3 ligand FL (138 nM/20 μl) largely inhibited acute morphine analgesia in $Flt3^{WT}$ mice (Fig. 3d), which was totally prevented by the intrathecal injection of PKI14-22 (Fig. S8). This demonstrates that FLT3 activation governs MOR functioning via cAMP signaling pathway. Altogether, our findings underscore the crucial role of neuronal FLT3 in the DRG in promoting OIT and OIH.

Pharmacological FLT3 inhibition improves morphine analgesia without aggravating morphine side effects

Building upon this groundwork, we aimed to leverage these findings with the idea of a new therapeutic approach combining the FLT3 specific inhibitor BDT001 and morphine. We hypothesized that this combination could provide better analgesia compared to morphine alone. We found that administering BDT001 (5 mg/kg, intraperitoneal) 90 min before morphine (2.5 mg/kg, subcutaneous) treatment significantly potentiated acute morphine analgesia in rats, as shown by the leftward shift in the morphine dose-response curve which represents a ~ 30% morphine-sparing effect (Fig. 4a, b). Similar results were obtained in mice (Fig. S9). We also show that administration of BDT001 totally prevented OIH and OIT in chronic morphine-treated rats (Fig. 4c, d). In addition, BDT001 alone did not induce constipation nor respiratory depression and did not affect the intensity or duration of these side effects when they were caused by chronic morphine in mice (Fig. 4e, f). Also, BDT001 did not exacerbate withdrawal responses precipitated by the opioid receptor antagonist naloxone following chronic morphine[38] (Fig. 4g). Importantly, in the conditioned place preference paradigm, BDT001 did not induce motivational effects, and

https://doi.org/10.1038/s41467-024-54054-y

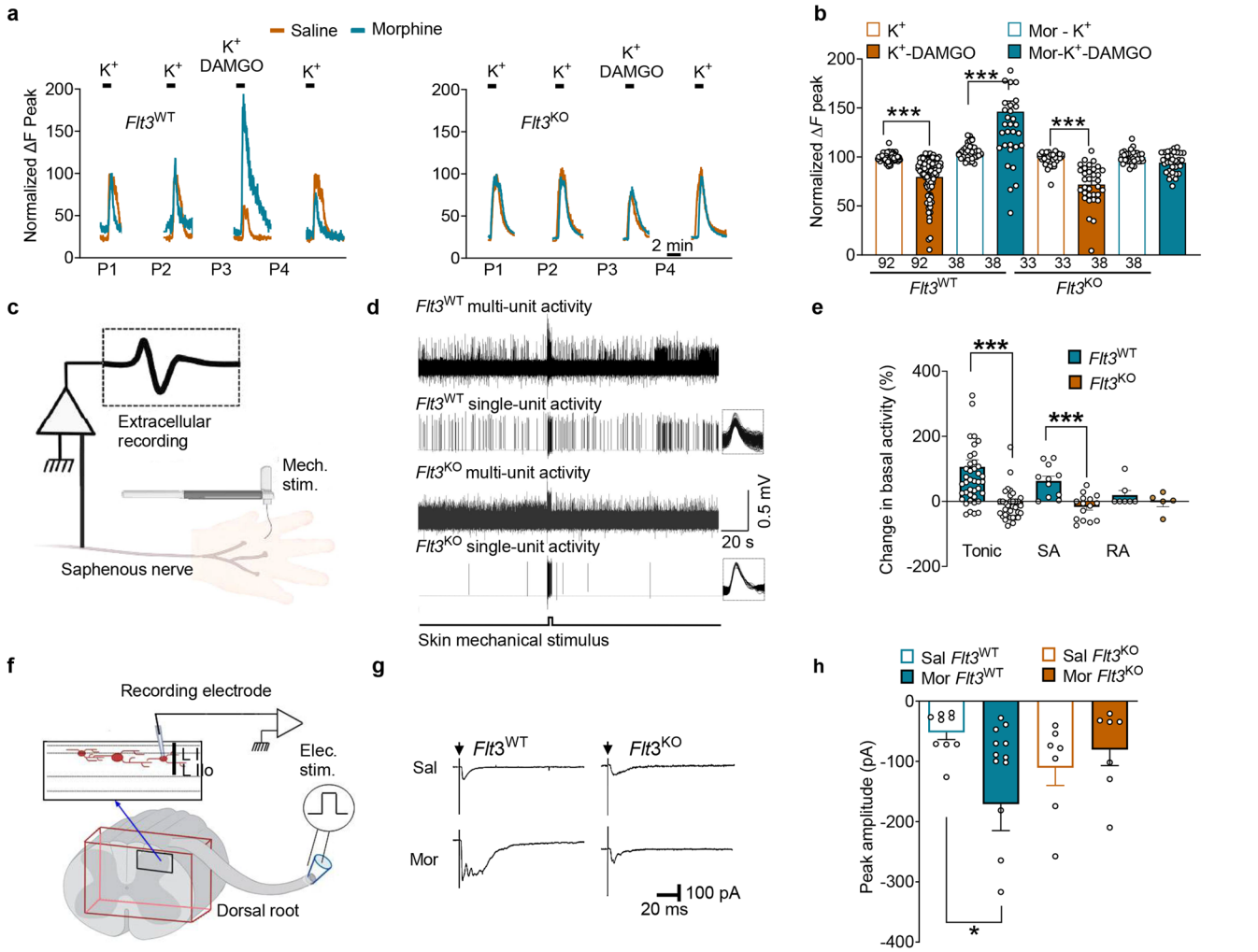

Fig. 2 | FLT3 controls chronic morphine-induced peripheral neuronal hyperexcitability in mice. a Traces of $[Ca^{2+}]_i$ responses to repeated bath applications of high K^+ (HiK^+, 50 mM) alone or combined with DAMGO (1 μM), in cultured DRG neurons from *Flt3*^{WT} ($n = 4$) or *Flt3*^{KO} ($n = 4$) mice treated with chronic saline or morphine (morphine at 10 μM for 3–4 DIV, followed by rinsing out). **b** Results are expressed as response amplitudes normalized to HiK^+ alone (ΔF peak). Data were obtained from more than three biologically independent experiments. To ensure clarity in the data representation, 3 points (216, 271 and 296%) were not displayed on the graph for the Mor-K^+-DAMGO/*Flt3*^{WT} group. The numbers below the X-axis indicate the total number of cells recorded for each group. **c** Scheme of the skin-nerve preparation set-up. **d** Ex vivo extracellular recordings of spontaneous- and mechanically evoked-activity on high threshold C-mechanoreceptors from saphenous-nerve preparations of *Flt3*^{WT} and *Flt3*^{KO} mice before and after a 10 s-mechanical stimulus (*bottom trace)* applied on mice treated with chronic morphine. **e** Normalized firing of cutaneous mechanoreceptors recorded in *Flt3*^{WT} ($n = 7$) or *Flt3*^{KO} ($n = 4$) mice exposed to chronic morphine ($p < 0.0001$ and $p = 0.0009$). To ensure clarity in the data representation, 3 points (450, 562 and 567%) were not displayed on the graph for Tonic *Flt3*^{WT} group. **f** Scheme of the electrophysiological set-up to record evoked responses in lamina I-IIo in the DHSC after electrical stimulatio of the dorsal root. **g** Examples of monosynaptic evoked responses induced by dorsal roots electrical stimulation (arrows) in spinal slices of *Flt3*^{WT} and *Flt3*^{KO} mice treated with either chronic saline or morphine. **h** Peak amplitude of monosynaptic evoked responses of neurons recorded from saline-treated *Flt3*^{WT} ($n = 6$) or *Flt3*^{KO} ($n = 6$) mice, and morphine-treated *Flt3*^{WT} ($n = 8$) or *Flt3*^{KO} ($n = 5$) mice ($p = 0.0477$). To ensure clarity in the data representation, 2 points (−406 and −585 pA) were not displayed on the graph for the Mor *Flt3*^{WT} group. Elec. stim, electrical stimulation; Mech. stim, mechanical stimulation; Mor, morphine; Sal, saline; Sc. Nerve, sciatic nerve; Tonic, high threshold C-type mechanonociceptors; RA, low-threshold rapidly-adapting mechanoreceptors; SA, low-threshold C-type slowly-adapting mechanoreceptors. LIIo: lamina II outer. Bars in (**b**, **e**, **h**) represent mean ± SEM of n neurons per group. $^*P < 0.05$, $^{**}P < 0.01$, $^{***}P < 0.001$. Statistical analyses included mixed-effects model (REML) followed by adjusted Bonferroni's test for multiple comparisons (**b, e**) and the Kruskal-Wallis test followed by adjusted Dunnett's test for multiple comparisons (**h**). Panel (**f**) was created in BioRender. Thouaye, M. (2024) BioRender.com/w51v287. Source data are provided as a Source Data file.

did not reveal a place preference in mice receiving a non-rewarding low dose of morphine (1.5 mg/kg; Fig. 4h). Hence, our findings show that the enhancement of morphine analgesia by BDT001 was not associated with an exacerbation of morphine adverse effects.

BDT001 in combination with morphine is effective in preventing and relieving acute and chronic pain

Because opioids are clinically prescribed to treat moderate to severe pain, we conducted experiments to evaluate the benefits of combining morphine and BDT001 therapy in two animal models of pain. For this purpose, we tested BDT001, alone or in combination with morphine, in mice with acute postsurgical pain, or rats with persistent inflammatory pain. Firstly, using the incisional postsurgical pain model in mice[39,40], we found that 24 h post-surgery, the pain threshold was strongly decreased to a similar extent in control animals and those treated with a low dose of morphine (1.5 mg/kg), indicating that the dose of morphine was ineffective (Fig. 5a). BDT001 alone, administered during the surgical procedure, had a partial but significant analgesic effect. Notably, morphine administration (1.5 mg/kg) to BDT001-treated mice induced a marked increase in the pain threshold (Fig. 5a), indicating

https://doi.org/10.1038/s41467-024-54054-y

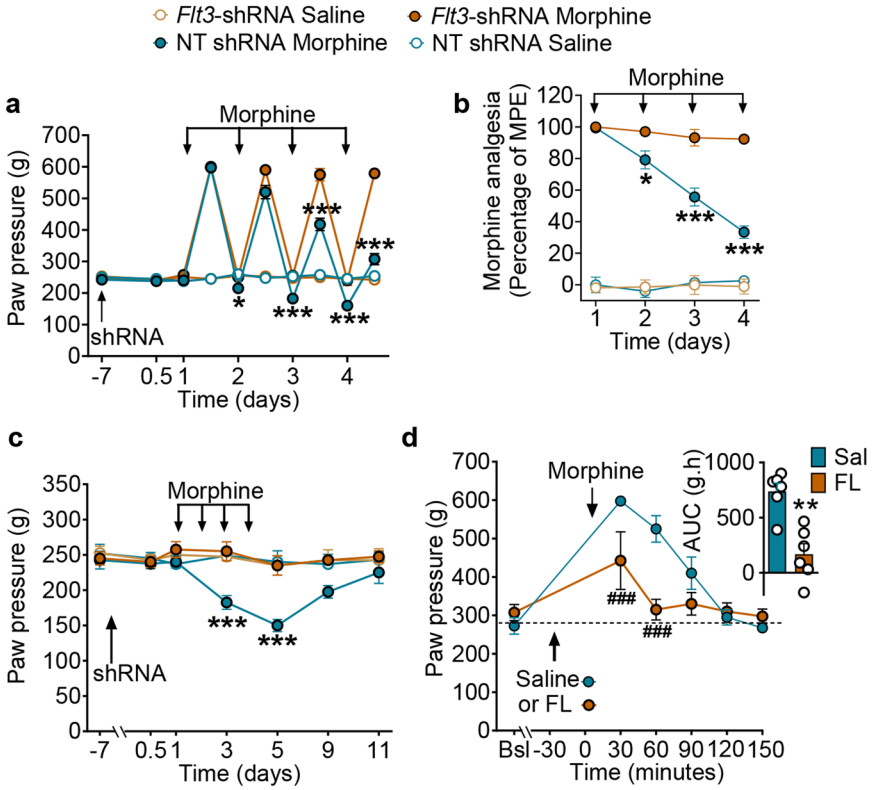

Fig. 3 | FLT3 expressed in rat DRG neurons is required for the onset of OIT and OIH. a Mechanical pain sensitivity of rats receiving a single intrathecal injection of AAV9 non-target (NT shRNA) shRNA or AAV9 *Flt3*-shRNA virus before and during chronic morphine (2 mg/kg twice a day for 4 days, subcutaneously) ($n = 5$–6 rats/group; $p = 0.0453$ and $p < 0.0001$). **b** Representation of anti-nociception as the percentage of Maximal Possible Effect (MPE) after the first daily injection of morphine in AAV9 non-targeted (NT shRNA) shRNA- or AAV9 *Flt3*-shRNA-treated rats ($p = 0.0293$ and $p < 0.0001$). **c** Mechanical pain sensitivity of rats receiving a single i.t. injection of AAV9 non-targeted shRNA or AAV9 *Flt3*-shRNA virus before daily morphine treatment. **d** Mechanical pain sensitivity of rats receiving a single intrathecal injection of FL (138 nM/20 µL) 30 min before an acute morphine injection (2 mg/kg, subcutaneously) ($n = 6$ rats/group). Inset: Bar and symbols represent mean of area under the curve (AUC; $p = 0.0043$). Data are shown as mean ± SEM $^*P < 0.05$, $^{**}P < 0.01$, $^{***}P < 0.001$ vs. NT shRNA; ### P < 0.001 vs. Saline. Statistical analyses included mixed-effects (REML) (**a**) or two-way ANOVA (**b**–**d**) followed by the adjusted Bonferroni's test for multiple comparisons and two-sided Mann-Whitney test for two unpaired comparison (**d**, *inset*). Source data are provided as a Source Data file.

that a synergistic drug combination might enable lower doses of morphine to be efficient. Secondly, the BDT001-morphine drug combination prevented OIH and OIT in the Complete Freund's Adjuvant (CFA) model[41] of persistent inflammatory pain in rats. As classically described, CFA injection into the hindpaw resulted in a decrease in mechanical pain thresholds (Fig. 5b, c and S10a, c). Animals subsequently receiving chronic morphine showed OIT (Fig. 5c, S10b) and OIH (Fig. 5b, S10c). Concomitant administration of BDT001 with morphine enhanced morphine analgesia and prevented morphine tolerance (Fig. S10a, b). The combination of morphine with BDT001 had modest effects on CFA-induced inflammation as evaluated by the diameter of the injected hindpaw (Fig. S10d), suggesting that the restoration of morphine analgesia was unlikely due to an action of BDT001 on peripheral inflammation. Finally, we conducted experiments to assess the curative effects of BDT001 on OIT and OIH (Fig. 5b–d). Rats received morphine alone, twice daily for four days (7 to 10 days post-CFA), until OIH and OIT were established. Morphine treatment was then combined with BDT001 in some animals from 11 to 14 days post-CFA. The baseline pain threshold, measured each day before the first morphine treatment, progressively normalized in animals treated with BDT001 (Fig. 5b), indicative of a reversal of OIH. The first injection of morphine (7 days post-CFA) produced a robust analgesic effect that decreased over the time with the repetition of the injections (Fig. 5c, d). Importantly, as soon as the first BDT001 injection was performed (11 days post-CFA), morphine analgesia was increased and entirely restored after 4 days of BDT001 treatment (15 days post-CFA) (Fig. 5c, d), indicative of a reversal of OIT. In summary, these results indicate that BDT001 therapy, in association with morphine, improves acute and chronic morphine analgesia in pain models by preventing or reversing OIT and OIH.

Discussion

The long-term use of opioids to maintain adequate pain relief in chronic pain is prevented by our lack of fundamental knowledge about the mechanisms limiting their efficacy over time. Since opioid-induced analgesia and side-effects appears controlled by different and specific mechanisms, identifying the actors involved in these processes appears adequate to find therapeutic strategies that would permit the chronic use of opioids without their adverse consequences. Our study provides insights on the critical implication of FLT3 expressed in DRG neurons, in OIT and OIH. Our findings reveal that FLT3 activation regulates the MOR-dependent canonical cAMP-PKA pathway, causing neuronal hyperexcitability that in turn drives the initiation of adverse counter-adaptations to opioid analgesia and facilitates the development of OIT and OIH. Thus, blockade of peripheral FLT3 prevents OIT and OIH while largely improving morphine analgesic efficacy in acute and chronic pain models (Fig. 6).

Several biochemical and cellular mechanisms participate in the development of OIH and OIT at different cellular or neuronal levels. In DRG neurons, the increased activity of the AC/cAMP/PKA pathway after chronic morphine treatment, referred to as 'superactivation' of AC, represents one of the key signaling systems which counteracts

https://doi.org/10.1038/s41467-024-54054-y

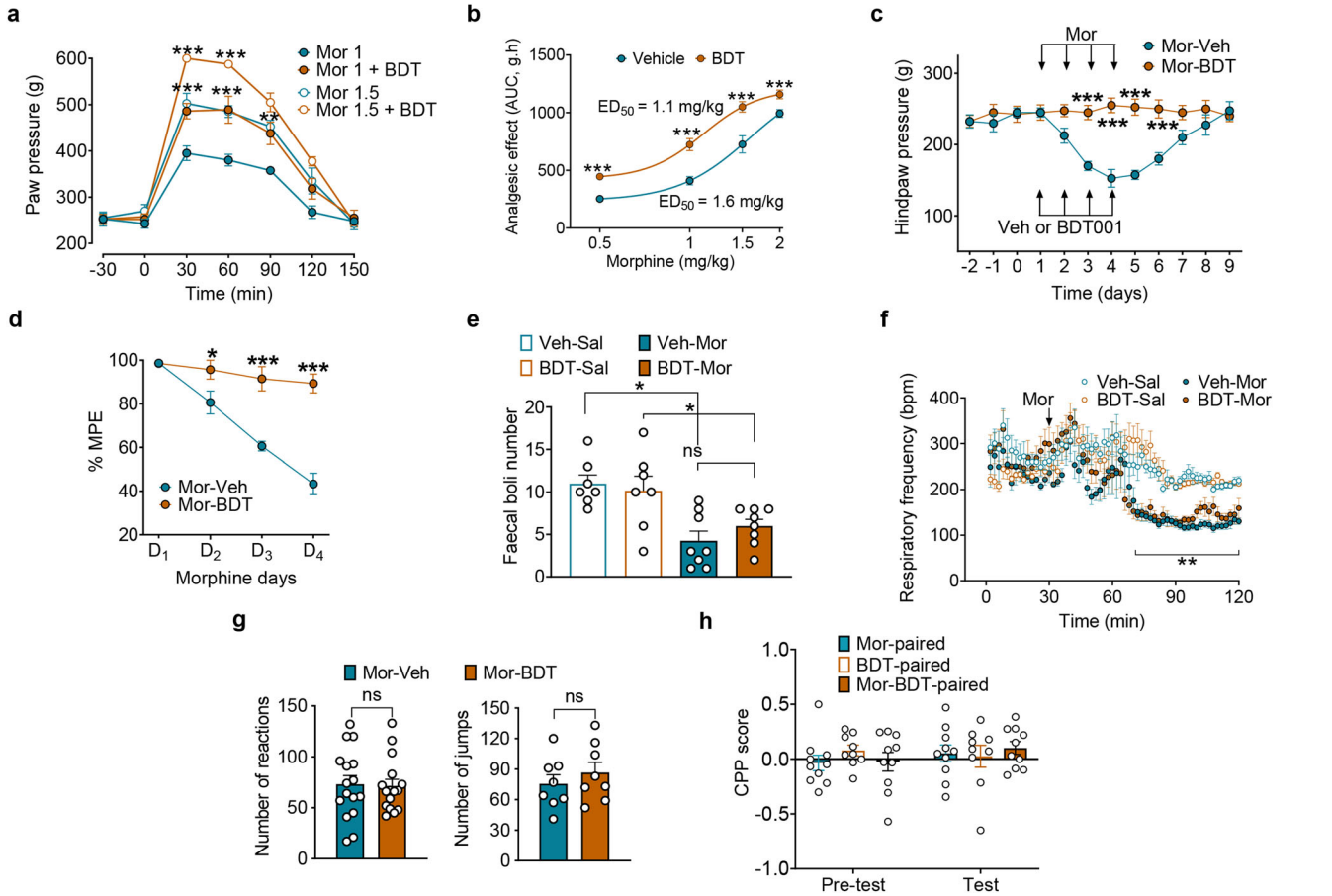

Fig. 4 | Pharmacological inhibition of FLT3 by BDT001 improves morphine analgesia without affecting morphine side-effects. a, **b** Dose-response curve of morphine (Mor) analgesia with or without pre-treatment with intraperitoneal (i.p.) BDT001 (BDT, 5 mg/kg) injected 90 min before subcutaneous (s.c.) morphine administration in rats ($n = 6$ rats/group). **c** Mechanical sensory sensitivity of rats receiving i.p. vehicle or BDT001 (5 mg/kg) 90 min before s.c. chronic morphine treatment (2 mg/kg, twice a day for 4 days) ($n = 6$ rats/group). **d** Measurement of morphine antinociception (percentage of MPE) during s.c. chronic morphine treatment ($n = 6$ rats/group; $p = 0.0456$). **e** Constipation in mice receiving i.p. vehicle or BDT001 (5 mg/kg) followed by s.c. saline or morphine (10 mg/kg) ($n = 8$ mice/group; $p = 0.0174$ and $p = 0.0299$). **f** Respiratory frequency in WT mice after s.c. saline or morphine injection with i.p. vehicle or BDT001 (5 mg/kg) ($n = 8$ mice/group). **g** BDT001 (5 mg/kg) did not enhance naloxone-precipitated withdrawal signs in chronic morphine mice ($n = 16$ mice/group for the number of reactions and $n = 8$ mice/group for the number of jumps). **h** BDT001 (5 mg/kg) had no motivational effects in mice and did not potentiate the motivational effects of a low, inactive dose of morphine (Mor 1.5 mg/kg) as evaluated with the conditioned place preference ($n = 9$–10 mice/group). Data are shown as mean ± SEM ($n = 10$–12 mice/group). $^{*}P < 0.05$, $^{**}P < 0.01$, $^{***}P < 0.001$ vs. morphine alone. Statistical analyses included two-way repeated ANOVA followed by adjusted Bonferroni's test for multiple comparisons (**a**–**c**), two-sided Mann-Whitney test (**d**), and two-way repeated ANOVA (**e**). BDT BDT001, Mor morphine, Sal saline, Veh vehicle. Source data are provided as a Source Data file.

the acute Gi/o protein coupling activities of MOR, promoting morphine-induced excitatory effects[35,42]. We confirmed in both in vitro and in vivo experiments that morphine excitatory effects depend indeed on the hyperactivation of AC, which promotes OIH. Strikingly, FLT3 deletion prevented the loss of morphine-induced inhibition on forskolin-induced cAMP increase in vitro (Fig. 1f) and in vivo (Fig. 1e), strongly suggesting that FLT3 regulates MOR excitatory effects via the AC/cAMP/PKA pathway. Our data further show that FLT3 inhibition reduced morphine-induced sensory neuronal hyperexcitability at peripheral and central presynaptic DRG/DSC synapse levels. First, in cultured DRG neurons exposed to chronic morphine, application of DAMGO increased HiK^{+}-induced $[Ca^{2+}]_i$ in culture collected from *Flt3*^{WT}, but not from *Flt3*^{KO} mice (Fig. 2a, b). In order to address some limitations associated with the Ca^{2+} imaging experiments, further investigation is needed to ascertain which sensory neurons derived from primary cultures express the FLT3 receptor. Second, our electrophysiological studies on skin-nerve preparation revealed the absence of post-discharges after mechanical stimulation of the saphenous nerve in chronic morphine-treated *Flt3*^{KO} mice as compared to morphine-treated *Flt3*^{WT} animals (Fig. 2d, e). Third, though the identity of cells recorded remains elusive, chronic morphine produced an increase in the peak amplitude of dorsal horn eEPSCs compared to chronic saline-treated mice, while *Flt3* deletion prevented morphine-induced spinal hyperexcitability (Fig. 2g, h). Biochemical analysis confirmed these functional studies. Indeed, in agreement with previous studies[28], chronic morphine induced the overexpression of neuronal hyperexcitability markers in DRG and spinal cord as shown with increased expression of CGRP in morphine-treated *Flt3*^{WT} mice in the DRG and the increased expression of glial (GFAP and Iba1) markers 5 days after the beginning of morphine treatment. Here again, the deletion of FLT3 prevented morphine-induced central sensitization as shown by the reduced expression of GFAP, Iba1 and CGRP in *Flt3*^{KO} mice in the spinal cord (Fig. 1g–j). Finally, at the behavioral level, targeting FLT3 in DRG using intrathecal AAV9-FLT3 shRNA virus[29] abolished OIT and OIH development, improving morphine analgesia (Fig. 3a–c). Conversely, FLT3 activation by FL dramatically reduced morphine analgesia suggesting a direct intervention of FLT3 on MOR signaling pathway supporting morphine analgesia (Fig. 3d). Hence, FLT3 signaling contributes to the molecular and synaptic changes in

https://doi.org/10.1038/s41467-024-54054-y

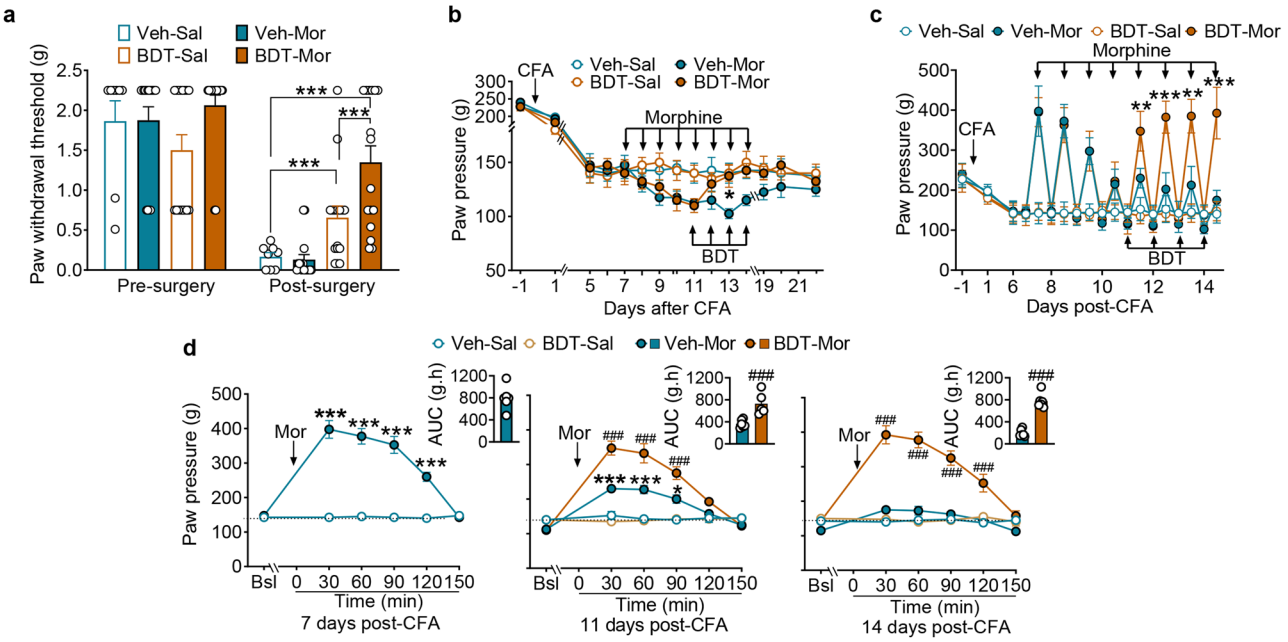

Fig. 5 | Pharmacological inhibition of FLT3 by BDT001 enhances morphine analgesia in acute pain and reverses tolerance in chronic inflammatory pain. **a** Effect of i.p. vehicle ($n = 8$), BDT001 (5 mg/kg; $n = 16$) alone or in combination with s.c. morphine (1.5 mg/kg; $n = 16$) on post-surgical pain in mice, before or 24 h after surgery. ($p < 0.0001$). **b** Curative effect of i.p. BDT001 (5 mg/kg) on OIH in CFA-treated rats ($n = 6$ rats/group, $p = 0.0434$). BDT001 treatment was initiated on the 5th day of morphine treatment, which was continued for 3 more days. **c** Morphine analgesia progressively decreased, as morphine-induced increase in mechanical pain thresholds vanished, as shown by the maximal morphine effect at 30 min. BDT001 treatment restored morphine analgesia ($n = 6$ rats/group, respective order on the graph $p = 0.0047$; $p < 0.0001$; $p = 0.0003$; $p = 0.0008$). **d** Time-course and AUC analysis (inset) of the morphine analgesic effect in rats combined with vehicle or BDT001 administration at 7, 11 and 14 days after CFA. Inset: Bar and symbols represent mean of AUC ± SEM of 6 rats per group. $^{*}P < 0.05$, $^{***}P < 0.001$ for the indicated comparisons (**a**); $^{*}P < 0.05$, $^{***}P < 0.001$ vs. Vehicle (Veh)-Saline (Sal) and ### P < 0.001 vs. morphine alone (**b**–**d**). Statistical analyses included two-way ANOVA (**a**–**c**) or mixed-effects (REML) (**d**) followed by adjusted Bonferroni's test for multiple comparisons and two-sided Mann-Whitney test (**d**, insets). Source data are provided as a Source Data file.

DRG neurons that induced the functional adaptation at the MOR level resulting in OIH and OIT.

Sustained peripheral and central alterations induced by chronic morphine treatment are abrogated by FLT3 deletion. A key concept emerging from our findings is the existence of a functional interaction between MOR and FLT3 receptors in peripheral DRG neurons, driving the initiation of adverse counter-adaptations to opioid analgesia, and allowing the onset of OIT and OIH. Other functional interactions between MOR and RTKs have been documented in heterologous expression systems or diverse native central neurons. Here, we identified a functional interaction between the G protein-coupled receptors MOR and the RTK FLT3 both at cellular and behavioral levels. Our results showed that MOR and FLT3 are co-localized in DRG neurons, and morphine treatment increased their co-localization in $FLT3^{+}$ cells, suggesting an increased functional interaction between MOR and FLT3 after chronic opioid exposure. On the one hand, in control animals, acute FLT3 activation by FL reduced (Fig. 3c) and FLT3 inhibition enhanced morphine analgesia (Fig. 4a, b). Importantly, in this case, FLT3 inhibition alone does not have any analgesic effect[29] suggesting that FLT3 inhibitors restore morphine-mediated analgesia rather than causing analgesia by themselves. These results also indicate a possible MOR-induced FLT3 activation that induces the activation of pronociceptive systems, thus counteracting morphine-induced analgesia. Such MOR/RTKs transactivation events have been identified at DRG and spinal cord levels where MOR functionally activates and interacts with PDGR[31] and EGFR[43], to modulate opioid-induced analgesia and take part in OIH and OIT. Two major pathways for RTK activation by MOR have been identified involving either extracellular RTK ligand release or intracellular effector signaling recruitment[44]. How FLT3 activation is MOR-dependent remains to be elucidated. On the other hand, RTKs can also transactivate MOR-mediated signaling that controls morphine tolerance development as well as OIH[45]. In the present study, FLT3 deletion prevented morphine-induced cellular and biochemical changes blunting both OIT and OIH and suggesting a key role for FLT3-MOR interaction in these adverse effects. Depending on the RTK and the cell-type studied, RTK-modulated MOR activations have been shown to involve different mechanisms, e.g. receptor physical interactions or intracellular pathway crosstalks[45]. Thus, delineating how FLT3 and MOR receptor co-regulate each other's activities and signaling pathways is an important subject for future research.

While opioids remain widely used in the treatment of post-operative and chronic inflammatory pain, their loss of efficacy with repeated dosing is positively correlated with dose escalation leading to an increase of morbidity and mortality, and are key contributors to the ongoing opioid crisis[5,46]. Thus, prospective therapeutic strategies need to alleviate dose escalation without decreasing opioid analgesia. Our results indicate that, in healthy and pathological conditions, inhibiting FLT3 signaling at the DRG level could limit dose escalation following chronic opioid exposure, while maintaining morphine analgesia. In this sense, we showed here that inhibiting FLT3 with BDT001, a specific negative allosteric modulator of FLT3 known to inhibit neuropathic pain-induced hyperexcitability[29], not only prevents morphine analgesic tolerance but also potentiates morphine analgesia in naive animals, resulting in ~30% reduction of the morphine dose producing the same analgesic effect (Fig. 4e; see leftward shift in the morphine dose-response curve). Because clinical opioid medication is typically associated with the relief of pain, we ascertain BDT001 therapeutic effects in both acute post-operative pain and chronic inflammatory pain. Importantly, BDT001 repeated injections yield stronger potentiation of morphine analgesia in these pain conditions (compared to naive), prevents the development (preventive effect) and once installed, drastically reverses (curative effect) tolerance and OIH (Fig. 5),

https://doi.org/10.1038/s41467-024-54054-y

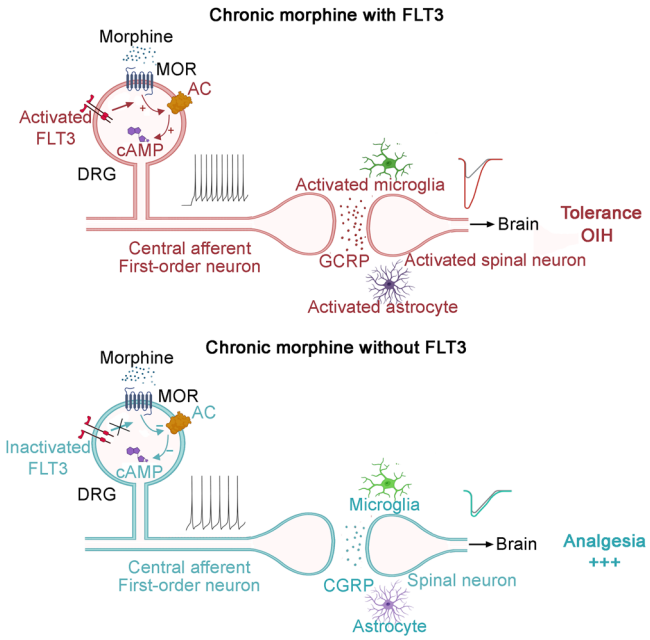

Fig. 6 | Schematic view of the functional interaction between MOR and FLT3 in DRG neurons promoting OIH and OIT. Chronic MOR stimulation produces excitatory effects at the DRG levels via the activation of FLT3 signaling in sensory neurons leading to neuronal hyperexcitability. That would promote over-expression of CGRP, glial activation and post-synaptic hyperexcitability in the dorsal horn of the spinal cord. All these molecular changes and synaptic changes support OIH and OIT. Blocking FLT3 activation inhibits chronic morphine-induced molecular and cellular excitatory changes restoring morphine analgesia. The figure was created in BioRender. Thouaye, M. (2024) BioRender.com/y65f560. AC Adenylate cyclase, DRG Dorsal root ganglia, cAMP Cyclic adenosine monophosphate, CGRP calcitonin gene-related peptide, FLT3 Fms-like tyrosine kinase 3, MOR μ opioid receptor, OIH Opioid-induced hyperalgesia.

improving morphine analgesia during treatment of chronic pain. In addition, BDT001 alone does not elicit the various morphine-induced side effects and does not potentiate these effects in combination with morphine as shown for respiratory depression, constipation and rewarding effects, three critical opioid-induced side effects (Fig. 4f–h). Therefore, targeting peripheral opioid receptor by modulating FLT3 expressed in DRGs appears a promising strategy to treat persistent pain.

To date, pain relief in humans suffering from cancer-associated chronic pain treated with an FLT3 inhibitor has been suggested in one clinical report[47]. In this study, patients with androgen-independent prostate cancer were treated by sorafenib, a potent FLT3 inhibitor (IC_{50} = 13 nM). Pain response, as measured by a two-point reduction in the Present Pain Intensity score (PPI, scored 1-5), without an increase in analgesic demand, or as a 50% or greater reduction in the analgesic demand without an increase in PPI, maintained for at least 3 weeks, was found in 15 patients out of 64. Among them, 3 stopped and 3 reduced by 75% the use of morphine. The results suggest a specific effect of sorafenib on pain and on opioid demand, rather than an indirect effect of tumor regression (14% and 78% of the patients have stable or slow progressive disease respectively). Nevertheless, the response rate of patients on analgesics was not reported in the publication. Interestingly, single-cell RNA sequencing analysis of human DRG neurons[48] show that *Oprm1* and *Flt3* mRNAs are present and co-expressed by the same neurons (Fig. S11). Altogether, these observations strongly suggest that such a functional interaction between MOR and FLT3 may occur in patients.

To conclude, our research shows that FLT3 expressed in primary afferent neurons regulates MOR function by altering MOR inhibitory properties following chronic opioid exposure. We propose that this process is conserved in mice and rats and, potentially in humans, driving the initiation of adverse counter-adaptations to opioid analgesia, allowing the development of OIT and OIH. Our research lays a scientific foundation for developing therapeutic strategies aimed at disrupting FLT3 signaling to maintain effective morphine pain relief during chronic morphine use. Specifically, BDT001 enhances morphine analgesia and prevents morphine tolerance in persistent inflammatory pain without exacerbating morphine's adverse effects. Therefore, FLT3 inhibitors, which prevent dose escalation without diminishing opioid analgesia, hold promise as potential agents to improve chronic opioid therapies. Ultimately, our fundamental findings highlight the exciting possibility that more effective treatments might soon be available for the countless patients suffering from chronic pain worldwide.

Methods

Animals

Experiments were performed in male *Sprague-Dawley* rats (150–170 g, Janvier, France), *C57BL/6* naive mice (25–30 g, Janvier, France), or *C57BL/6* mice carrying a homozygous deletion of Flt3 (*Flt3*^{KO} mice) and their littermates (WT) weighing 25–30 g. All the procedures were approved by the French Ministry of Research (authorization # 20114-2019040310181741v3). Animals were maintained in a climate-controlled room on a 12 h light/dark cycle and allowed access to food and water ad libitum. Housing conditions were maintained at a temperature of 22–23 °C and a humidity level of 40–50%. For rats and mice, we used n = 6 or 8 per group for each experiment respectively, otherwise the number is noted in the legends. Male and female mice were first considered separately in behavioral procedures. Both sexes showed mechanical hypersensitivity of same intensity after repeated morphine injection and were similarly affected by *Flt3* deletion (ANOVA followed by Bonferroni's test, n = 8 for both sexes and genotypes for each experiment, Fig. S1). Thereafter, experiments were performed only on male mice.

Drug delivery

Opioids. Morphine HCl was purchased from Francopia, dissolved in 0.9% sodium chloride and administered subcutaneously. For the chronic morphine administration protocol, morphine subcutaneous injections were performed twice a day with 8 h of interval during 4 days. Rats and mice received 2 mg/kg and 10 mg/kg per injection, respectively. For acute morphine-FL treatment protocol in rats one subcutaneous morphine injection (2 mg/kg) was performed 30 min after FL (138 nM/20 μl) intrathecal injection.

FL. Human recombinant FL (FLT3 ligand) was obtained in the E. coli Rosetta (DE3) strain (Novagen) in our laboratory using the pET15b-rhFL plasmid and was dissolved in saline solution. For recombinant FL intrathecal injection, a 30 G needle attached to a Hamilton syringe was inserted between L4 and L5 vertebrae in lightly restrained, isoflurane-anaesthesized rats. The reflexive tail flick was used to confirm the punction. A total volume of 20 μl was injected.

PKA pharmacological inhibitor. One hour before intrathecal injection of FL, the PKA inhibitor PKI 14-22 (#2546 – Tocris) was administered intrathecally at a concentration of 5 μg/10 μl.

BDT001. BDT001 was synthesized at Laboratoire d'Innovation Thérapeutique (UMR7200, CNRS – Université de Strasbourg, Illkirch 67400 France)[29]. BDT001 was dissolved in 7% Tween 20 in a saline solution with 6 sonication runs of 45 se. BDT001 was injected at 5 mg/kg in mice and at 2 mg/kg in rats. For chronic morphine protocol with BDT001 treatment in rat, intraperitoneal injection of BDT001 was performed 2 h before the morning morphine injection.

Pain model

Inflammation. The model of complete Freund's adjuvant (CFA)-induced pain has been used for assessing chronic inflammatory pain in rat as described before[41]. Once CFA-induced hypersensitivity was established, chronic morphine administration was performed as described above. For preventive experiments, morphine and BDT001 administration started on the same day for 4 days. For the curative experiments, chronic morphine was first administered and once analgesic tolerance and morphine-induced hyperalgesia was established, BDT001 treatment was started with the following morphine injections.

Paw incision models. *C57BL/6 J* mice were anesthetized under isoflurane (3% vol/vol) and the hindpaw was incised as previously described[39]. BDT001 or vehicle was administered 90 min before the incision. On D1, a single saline or morphine injection (1.5 mg/kg; i.p.) was administered and the nociceptive threshold was evaluated 30 min later.

Behavioral analysis

Before testing, rats and mice were acclimatized for 60 min in the temperature and light-controlled testing room within a plastic cylinder or on wire mesh. Experimenters were blinded to the genotype or the drug administered. Since acute active morphine injection induce motor hyperactivity in mice but not in rats, we chose rats to study morphine analgesia in details to obtain a better temporal assessment of the analgesia by repeated (every 30 min) measurements of the morphine effect.

Tactile sensitivity. Tactile withdrawal threshold was determined in response to probing of the hindpaw with eight calibrated von Frey filaments (Stoeling, Wood Dale, IL, USA) in logarithmically spaced increments ranging from 0.04 to 8 g (4–150 mN). The 50% paw withdrawal threshold was determined in grams by the Dixon nonparametric test[49]. The protocol was repeated until three changes in behavior occurred. This method was used in both rats and mice with adapted filaments.

Paw pressure test. To assess mechanical sensitivity in rats, a variant method of the Randall-Selitto method was performed[50] in which a continually increasing pressure is applied to the hind paw until the rat squeaks. The Basile analgesimeter (Apelex, Massy, France; stylus tip 1 mm in diameter) was used. To assess morphine analgesia, measurements were performed 30 min after morphine injection and in some experiments, the time course of morphine analgesia was determined by measuring nociceptive threshold every 30 min for 2h30 until return to a basal nociceptive threshold. To assess OIH, basal nociceptive threshold was assessed once daily before twice daily morphine administration.

Morphine and BDT001 motivational effects. To evaluate morphine or BDT001 motivational effects, a 5 days CPP protocol was set. The apparatus (Bioseb, France) consists in 2 chambers (size 20 cm x 18 cm x 25 cm) distinguished by the texture of the floor and by the wall patterns connected to each other by a central chamber (size 20 cm × 7 cm x 25 cm). During the first day, all the mice were able to move freely during 15 min in the whole apparatus. Their moves were recorded with a camera connected to Ethovision software. Mice with a spontaneous preference up to 75% were removed from the experiment. The next 3 days are the conditioning days. The morning, mice were restricted for 20 min to one chamber after morphine (1.5 mg/kg) or BDT001 (5 mg/kg) intraperitoneal injection. The afternoon, mice were again restricted for 20 min to the opposite chamber after vehicle intraperitoneal injection. Injections were switched off the next day in order to avoid time dependent conditioning. To evaluate the effects of BDT001 on morphine-induced motivational effects BDT001 or vehicle was administered in combination with morphine 2 h before morphine or saline conditioning. The 5th day is the test day. Mice were placed in the center chamber with free access to all chambers and the time spent in each chamber was recorded for 15 min. The preference scores were expressed as the difference between the time spent in the morphine- and/or BDT001-paired chamber and the vehicle-paired chamber.

Morphine side effects. Respiratory depression measurement using whole body plethysmography ventilatory parameters were recorded as previously described[49] in conscious *C57BL/6 N* mice by whole-body barometric plethysmography (Emka Technologies, Paris, France). Respiratory frequency (f) was recorded for 100 min and used as the index of respiratory depression. Accumulated faecal boli quantification was performed in *C57BL/6 J* mice[11]. The animals were subcutaneously injected with vehicle or BDT001 (5 mg/kg) and 1.5 h later they received saline or morphine (10 mg/kg) and individually placed into small Plexiglas boxes lined with filter paper. Faecal boli were collected and weighed every hour for 5 h after the drug injections.

Physical dependence studies. After induction of chronic tolerance, withdrawal was precipitated by 1 mg/kg naloxone hydrochloride injection performed 2 h after the last injection of morphine. Mice were individually placed in small Plexiglas boxes and observed and scored for 20 min for manifestation of different withdrawal signs, including jumping, grooming, rearing, forepaw shaking, genital licking and wet-dog shakes. A global withdrawal score, excluding weight loss, was calculated[38]. The sum of all weighted signs produced a global withdrawal score for each mouse.

Virus transfection

The following oligonucleotides were used to build the AAVGFP-shRNA plasmids: shFLT3 (GATCGGTGTCGAGCAGTACTCTAAATCAAGAGTTTAGAGTACTGCTCGACACCTTTTT(top)); AGCTAAAAAGGTGTCGAGCAGTACTCTAAACTCTTGATTTAGAGTACTGCTCGACACC(bottom); Sigma-Aldrich (TRC000000378670); non-targeted sh (GATCCAACAAGATGAAGAGCACCAATCAAGAGTTGGTGCTCTTCATCTTGTTGTTTTT (top)); AGCTAAAAACAACAAGATGAAGAGCACCAACTCTTGATTGGTG CTCTTCATCTTGTTG (bottom).The oligonucleotides were annealed and cloned BamHI–HindIII in a vector containing the U6 promoter sequence and the hGH polyadenylation sequence upstream and downstream, respectively, of the BamHI site. The U6-shRNA-hGH sequences were then cut using PmlI and HpaI and cloned in the pAAV-CMV-turbo GFP vector (Cell Biolabs Inc.) linearized with PmlI. All the constructs were checked by DNA sequencing. The viruses were produced by the Viral Vector Production Unit of Institut de la Vision, Paris, France. For in vivo experiments, 10 µl of AAV-turbo GFP-sh *Flt3* or AAV-turbo GFP- sh control solution were intrathecally injected in lightly restrained, unanaesthetized rats, as described above. The titer of the virus solution was 5.8×10^{12} genome copies (gc)/ml.

Adult sensory neuron culture

Neuron cultures were established from lumbar (L4–L6) dorsal root ganglia[29]. Briefly, ganglia were successively treated by two incubations with collagenase A (1 mg/ml, Roche Diagnostic, France) for 45 min each (37 °C) and trypsin-EDTA (0.25%, Sigma, St Quentin Fallavier, France) for 30 min. They were mechanically dissociated through the tip of a fire-polished Pasteur pipette in neurobasal (Life Technologies, Cergy-Pontoise, France) culture medium supplemented with 10% fetal bovine serum and DNase (50 U/ml, Sigma). Isolated cells were collected by centrifugation and suspended in neurobasal culture medium supplemented with 2% B27 (Life Technologies), 2 mM glutamine, penicillin/streptomycin (20 U/ml, 0.2 mg/ml) plated at a density of 2500 neurons per well in 96-well plates and were incubated in a humidified 95% air-5% CO2 atmosphere at 37 °C.

cAMP activation measurement by cAMP time-resolved FRET assays

Measurement of cAMP accumulation was performed using the cAMP-Gi immunoassay kits (Cisbio Bioassays) according to the manufacturer's instructions. Cultured adult sensory neuron cells were tested at 8 DIV after seeding in a 96-well plate. Briefly, for acute treatment, the cells at 8DIV, were pretreated with the indicated concentrations of CTAP (#C6352 - Sigma-Aldrich) for 20 min at 37 °C and stimulated 15 min at 37 °C with 10 μM of morphine (Francopia) in Stimulation Buffer containing 0.5 mM of IBMX (#I7018 – Sigma-Aldrich), prior the addition of 0.1 μM of forskolin (#F6886 - Sigma-Aldrich) during 15 min at 37 °C. The reaction was stopped by lysis buffer containing HTRF® assay reagents: the Europium Cryptate-labeled anti-cAMP antibody and the d2-labeled cAMP. The plate was then incubated for 1 h at room temperature before reading the fluorescence emission at 620 and 665 nm using a PHERAstar FS plate reader (BMG Labtech). In these conditions, acute morphine reduced forskolin-stimulated cAMP levels in DRG primary cultures from *Flt3*^{WT} mice and CTAP, a MOR-selective antagonist, blocked the inhibitory effects of morphine-induced inhibition of cAMP production by 95.45% ± 2.26 ($n = 11$; $p < 0.05$, one-way ANOVA followed by Bonferroni's test for multiple comparisons), indicating a MOR-dependent mechanism of morphine inhibition.

For chronic treatment, the cells were treated every day with 10 μM of morphine, 24 h after seeding in a 96-well plate and during seven days. At 8DIV, the same treatment protocol as that of the acute treatment was used to determine of the cAMP accumulation in DRG neurons.

For the measurement of cAMP accumulation in DRG, mice were treated with the saline buffer or morphine at 10 mg/kg in I.P twice a day during 3 days. The last day, Forskolin (FSK) was administrated at 1.5 μg intrathecal to stimulate adenylate cyclase. After 30 min, DRG (L1-L6) were collected, lysed and homogenized in the MagNA Lyser Instrument (Roche; twice for the speed of 6000 for 30 s) with ceramic spheres (Lysing Matrix D, MP Biomedicals, #116913100) in lysis & detection buffer 8 (64CL8FDD - Cisbio Bioassays) supplemented with complete protease inhibitor cocktail (Sigma-Aldrich #P8340) and 0.5 mM of IBMX (#I7018 – Sigma-Aldrich). Then, centrifugation (10 600 g for 15 min at 4 °C) was performed. Supernatants were collected and cAMP accumulation was measured as described above.

Real-Time qRT-PCR

Flt3^{WT} and *Flt3*^{KO} mice lumbar (L4–L6) dorsal root ganglia were dissected. RNA was extracted using the RNAqueous-4PCR Kit (Ambion) according to the manufacturer's protocol. The Real-Time qRT-PCR experiment has been described previously[29]. Sequences of the primer pairs (Sigma-Aldrich) used are as follows:

Polr2j: F-ACCACACTCTGGGGAACATC, R-CTCGCTGATGAGGTC TGTGA; NM_011293; *Ddx48*: F-GGAGTTAGCGGTGCAGATTC, R-AGC ATCTTGATAGCCCGTGT; NM_138669; *Flt3*: F- ATCCCCAGAAGACCT CCAGT, R- CTGGGTCTCTGTCACGTTCA; NM_010229.2; *Oprm1*: F- AC AGGCAGGGGTCCATAGAT, R- AATACAGCCACGACCACCAG; NM_0 01304948.1

Calcium imaging on cultured DRG neurons

For calcium imaging video microscopy [Ca^{2+}]i fluorescence imaging, DRG neurons were loaded with fluorescent dye 2.5 μM Fura-2 AM (Invitrogen, Carlsbad, CA) for 30 min at 37 °C in standard external solution contained: 145 mM NaCl, 5 mM KCl, 2 mM $CaCl_2$, 2 mM $MgCl_2$, 10 mM HEPES, 10 mM glucose (pH adjusted to 7.4 with NaOH and osmolarity between 300 and 310 mOsm). The coverslips were placed on a stage of Zeiss Axiovert 200 inverted microscope (Zeiss, München). Observations were made at room temperature (20–23 °C) with a 20X UApo/340 objective. Fluorescence intensity at 505 nm with excitation at 340 nm and 380 nm were captured as digital images (sampling rates of 0.1–2 s). Regions of interest were identified within the soma from which quantitative measurements were made by re-analysis of stored image sequences using MetaFluor Ratio Imaging software. [Ca^{2+}]i was determined by ratiometric method of Fura-2 fluorescence from calibration of series of buffered Ca^{2+} standards. Neurons were distinguished from non-neuronal cells by applying 50 mM KCl (HiK^+), which induced a rapid increase of [Ca^{2+}]i only in neurons. Only neurons with resting 340/380 fluorescence intensity ratio of 0.25–0.75 were included. We selected primary sensory neurons with small diameters which are known to be nociceptors and to contain MOR-expressing nociceptor subpopulation. Pulses of (50 mM) were applied at around 2 min-intervals and DAMGO (10 μM) was added after the third pulse. After DAMGO application, another HiK^+ stimuli was done to demonstrate recovery of the drug. All drugs and solutions were applied with a gravity-driven perfusion system. For chronic treatment, the cells were incubated either morphine (10 μM) or morphine and BDT001 (1 μM) during at least 72 h, with the solution renewed twice a day. For data analysis, amplitudes of [Ca^{2+}]i increases, ΔF/Fmax, caused by stimulation of neurons with HiK^+ were measured by subtracting the 'baseline' F/Fmax (mean for 30 s prior to HiK^+ perfusion) from the peak F/Fmax achieved on exposure to HiK^+. In the absence of any treatment, the distribution of these ratios was well fitted by a normal distribution. The DAMGO- induced [Ca^{2+}]I transient were expressed as a percentage of the average peak produced by the two previous HiK^+ stimuli. To avoid variations, control and drug treatment values were collected from the same cell. Data were collected from at least three different preparations.

Immunohistochemistry

Mice were transcardially perfused with PBS for all experiments DRG (L4-L6), spinal cord (lumbar segment), were collected and post-fixed in 4% paraformaldehyde between 10 min and 2 h depending on the antibody and tissue before being cryoprotected in 30% sucrose in PBS. Tissues were then frozen in O.C.T (Sakura Finetek). Sections (12 μm) were prepared using the Cryostat Leica CM2800E. For immunostaining, frozen sections were blocked and permeabilized in Ca^{2+}/Mg^{2+}-free PBS (PBS 1× −/−) containing 10% donkey serum and 0.1% or 0.3% Triton x-100 during 30 min. The sections were then incubated with primary antibodies, at 4 °C overnight in PBS 1× −/− containing 1% donkey serum and 0.1%, 0.01, or 0.03% Triton x-100. After extensive wash in PBS 1× −/− (3 times for 10 min minimum each) sections were incubated with appropriate secondary antibody, in the same buffer as the primary antibodies, at room temperature for 1 h and then washing (three times for 15 min each) before mounting with Mowiol. Images were acquired under a Zeiss slide scanner Axio Scan Z.1 for quantification and under Zeiss LSM 700 Confocal microscope for illustration with ZEN software (Carl Zeiss Microscopy). The following primary antibodies were employed: anti-CGRP Abcam ab36001 (goat 1:1000), anti-GFAP Abcam ab4674 (chicken 1:1000), anti-Iba1 Wako (rabbit 1:500). The following secondary antibodies were used anti-rabbit AlexaFluor 555/488/647 (donkey 1:1000), anti-goat AlexaFluor 488 (donkey 1:1000) from Life Technologies.

The quantification of CGRP immunostaining in DRG neurons was realized by counting the number of cells expressing CGRP. Ratio with total neuron number was done in different conditions, and results were expressed in mean of obtained ratios (± SEM) and statistical significance was determined by variance analysis (ANOVA one-way) followed by Bonferroni post-hoc test. The number of neurons expressing the various molecular markers of sensory neurons (subtypes) was determined by counting cells with NeuN immunostaining. A minimum of six sections from lumbar DRG were counted from at least 6 animals for each genotype. For Iba1, GFAP and CGRP the quantification was assessed by determining staining surface among spinal cord dorsal horns with ImageJ software, after setting a density threshold above background. Results were shown in mean (± SEM) and statistical significance was determined by variance analysis

(ANOVA one-way) followed by Bonferroni post-hoc test. A minimum of 5 sections of dorsal horn were quantified from at least 4 animals per condition.

In situ hybridization

Slides containing DRG sections (12 μm) were originally imaged for endogenous mCherry fluorescence and then submitted to in situ hybridization[51]. Briefly, sense and antisense digoxigenin (DIG)-labeled RNA probes were generated from a mouse *Flt3* cDNA clone (IRAMp995N1310Q, Genome-CUBE Source Bioscience) in a 20 μl reaction containing 1 μg of linearized plasmid (digested with HindIII and NheI, respectively) using the DIG RNA labelling mix (Roche Diagnostics) and T7 and Sp6 RNA polymerases respectively (Promega) following the manufacturer's instructions. DIG-labeled RNA probes were purified on MicroSpin G50 columns (GE Healthcare). L4–L6 lumbar dorsal root ganglia were dissected in phosphate-buffered saline (PBS), and fixed for 1 and 3 h, respectively, in 4% paraformaldehyde (PFA) at room temperature. Tissues were rinsed twice in PBS before immersion overnight in 25% sucrose/PBS at 4 °C. Slides were imaged in bright field. Image acquisition was done using a Hamamatsu NanoZoomer using NDP view software. The photographs were then taken for comparison with those showing the mCherry results on the same sections. The mCherry signals were converted into pseudo-red and the *Flt3* probes signals into pseudo-green fluorescent color. The pseudo-red fluorescent images were then carefully overlaid with pseudo-green fluorescent images. This sequential approach permits unequivocal identification of coexpression at the single cell level. Finally, neurons positive for each or both channels were manually counted.

Skin nerve preparation and ex vivo electrophysiological recordings

The in vitro glabrous skin-nerve preparation used was adapted from Zimmermann et al. [52] and described in Hao et al. [53]. Briefly, adult male mice were euthanatized using an overdose of isoflurane (Piramal, UK) followed by a method of confirmation of euthanasia. The saphenous nerve and the skin of the hind limb were carefully dissected and placed in a custom-designed organ chamber (INT-CFMN, Aix-Marseille University, Marseille, France) containing warm oxygenated Synthetic Interstitial Fluid (SIF buffer; 30.5 °C). The SIF buffer had the following composition (in mM): 120 NaCl, 3.5 KCl, 0.7 $MgSO_4$, 1.7 NaH_2PO_4, 5 Na_2HCO_3, 2 $CaCl_2$, 9.5 Na-Gluconate, 5.5 glucose, 7.5 sucrose, and 10 HEPES. The pH was set to 7.4 and the osmolarity was maintained at 300 mOsm/L. The skin was placed with the corium side up in the organ bath and the saphenous nerve was placed in an adjacent recording chamber filled with mineral oil. The skin was continuously superfused with oxygenated SIF buffer at a temperature of 30.5 °C controlled with a CL-100 temperature controller (Warner Instrument, Harvard apparatus, USA). The saphenous nerve was kept in a recording chamber filled with mineral oil, gently teased, and groups of nerve fibers were placed on the gold recording electrode in order to isolate single-unit activity. Then, extracellular action potentials from single nerve fibers were recorded with an AC differential amplifier DAM 80 (WPI) and converted digitally using the CED Spike2 system (sampling rate of 20 kHz; Cambridge Electronic Design, UK). Spikes were discriminated off-line with the Spike2 software (Cambridge Electronic Design Limited, UK) and analyzed individually to avoid false positives. Mechanical-threshold of single saphenous nerve fiber was obtained by probing the skin flap with von Frey hairs (Friedrich-Alexander University, Erlanger, Germany). Nociceptors were probed for their high threshold (> 16 mN) and tonic discharges during long lasting mechanical stimulation. Low-threshold mechanoreceptors (potential non nociceptors) were defined as having mechanical threshold below 5.7 mN and rapidly or slow adapting discharges. Once a fiber has been characterized, a single 10 s-supraliminar mechanical stimulation of the receptive field was applied using a von Frey filament mounted on the arm of a computer-controlled piezoelectric stepper (PI E-861 Nexact® controller; Germany). The post-discharge (or afterdischarge) was defined as a prolonged activity occurring within a 5 min-period after the end of the mechanical stimulus. Ratio of firing rates determined 5 min after the stimulus (post-discharge) and 5 min before the stimulus was used to analyze the post-discharge.

Slices preparation, electrophysiological recordings and stimulation

Adult male mice (3 to 6 weeks) were euthanatized with an intraperitoneal (i.p.) overdose of chloral hydrate (7 %). After a laminectomy, the thoraco-lumbar (T11-L3) spinal cord were removed and placed into an ice-cold sucrose-based saline solution containing the following (in mM): 2 KCl, 0.5 $CaCl_2$, 7 $MgCl_2$, 1.15 NaH_2PO_4, 26 $NaHCO_3$, 11 glucose, and 205 sucrose bubbled with 95% O_2, 5% CO_2. Transverse slices (550 μm thick) with attached dorsal roots obtained using a vibratome (VT1200 S, Leica Microsystèmes SAS, France) were incubated at 37 °C in artificial cerebro-spinal fluid solution containing (in mM): 130 NaCl, 3 KCl, 2.5 $CaCl_2$, 1.3 $MgSO_4$, 0.6 NaH_2PO_4, 25 $NaHCO_3$, 10 glucose (pH 7.4) and bubbled with 95 % O_2 and 5 % CO_2. After a 40 min recovery period, electrophysiological recordings were performed. Substantia gelatinosa neurons were visualized in spinal cord slices using an upright microscope fitted with fluorescence optics (AxioExaminer, Carl Zeiss, Germany) and linked to a digital camera QImaging Exi Aqua (Czech Republic). The lamina II was divided into outer (IIo) and inner (IIi) equal parts from the dorsal to ventral boundaries. Recorded lamina I and IIo interneurons were visualized using a 63x water immersion objective lens with combined infrared and differential interference. Patch pipettes (6–8 MΩ resistance) made from borosilicate glass (1.5 mm O.D; PG150T-15; Harvard Apparatus, UK) were filled with an internal solution containing (in mM): 127 K-gluconate, 4 NaCl, 2$MgCl_2$, 10 HEPES, 0.5 EGTA, 2.5 Na_2ATP, 0.5 Na_2GTP, 0.05% neurobiotin (Vector Laboratories), 0.01% dextran tetramethylrhodamine (10,000 MW, fluoro-ruby, Life technologies), pH 7.4 and osmolarity 290–300 mOsm. Whole-cell patch-clamp recordings were performed using Clampex 10 software connected to a Multiclamp 700B amplifier via a Digidata 1440 A digitizer (Molecular Devices, Sunnyvale, CA, USA). The sampling rate was 10 kHz, and the data were filtered at 3 kHz. Series resistance was monitored throughout the experiments and data were discarded if series resistance varied more than ± 20 MΩ. In voltage-clamp mode, neurons were clamped at −65 mV and evoked-postsynaptic currents (eEPSCs) were obtained by stimulating (5 pulses, 0.1 ms, 0.05 Hz, 500 μA) the dorsal root attached with a suction electrode. Monosynaptic eEPSC were determined based on three criteria: constant short latency, a smooth waveform with a jitter up to 2 ms and consistent responses without failure to repeated stimuli[54].

Statistical analysis

All experiments were randomized. All experiments involving animal behavior were randomized into groups that result in equal sample sizes. Briefly, baseline values were averaged and classified in ascending order. Animals were then successively assigned to a different experimental group. Data are expressed as the mean ± SEM. All sample sizes were chosen based on our previous studies except for animal studies for which sample size has been estimated via a power analysis using the G-power software. The power of all target values was 80% with an alpha level of 0.05 to detect a difference of 50%. Statistical significance was determined by analysis of variance (ANOVA one-way or two-way for repeated measures, over time), followed by Bonferonni's post-hoc test for multiple comparisons or uncorrected Fisher's LSD. Statistical analyses included also mixed-effects model (REML) followed by Bonferroni's test for multiple comparisons, the Kruskal-Wallis test followed

by Dunnett's test for multiple comparisons to a control group. To quantitatively evaluate morphine analgesic tolerance (MIT), the % maximal possible effect (%MPE) was evaluated by normalization of nociceptive threshold values during analgesia on Randall-Selitto cut-off value, as following: [(nociceptive threshold value 30' after morphine injection) − (basal nociceptive threshold)] ÷ [(cut-off value) − (basal nociceptive threshold)]. To quantitatively evaluate morphine analgesia, the area under the curve (AUC) was determined as following. The surface areas were calculated by summing the nociceptive threshold values measured every day after the planned day of experimentation, as follows: Surface area = Σ (nociceptive threshold values at H + n) − basal value × n, where n is the number of intervals. This total value is proportional to the surface area because the intervals between successive tests were similar (30 min). The results were expressed as a mean percentage (± SEM) of the reference AUC defined as the AUC calculated in morphine group alone (100% = AUC of morphine group). In this representation with unpaired data and without repeated measures, Mann-Whitney tests were performed to evaluate results statistical significance. To determine EC50 of morphine in presence of Vehicle or BDT001, a sigmoidal dose-response curve was generated with GraphPad Prism software (GraphPad Software, Inc., San Diego, USA) based on AUC raw data.

Reporting summary

Further information on research design is available in the Nature Portfolio Reporting Summary linked to this article.

Data availability

All data supporting the findings of this study are available within the paper and its supplementary information. Source data are provided with this paper.

References

1. Noble, M. et al. Long-term opioid management for chronic non-cancer pain. *Cochrane Database Syst. Rev*. **2010**, CD006605 (2010).
2. Rivat, C. & Ballantyne, J. The dark side of opioids in pain management: basic science explains clinical observation. *Pain Rep*. **1**, e570 (2016).
3. Roeckel, L.-A., Le Coz, G.-M., Gavériaux-Ruff, C. & Simonin, F. Opioid-induced hyperalgesia: Cellular and molecular mechanisms. *Neuroscience* **338**, 160–182 (2016).
4. Bekhit, M. H. Opioid-induced hyperalgesia and tolerance. *Am. J. Ther*. **17**, 498–510 (2010).
5. Stein, C. New concepts in opioid analgesia. *Expert Opin. Investig. Drugs* **27**, 765–775 (2018).
6. Christie, M. J. Cellular neuroadaptations to chronic opioids: tolerance, withdrawal and addiction. *Br. J. Pharmacol*. **154**, 384–396 (2008).
7. Corder, G. et al. Loss of μ opioid receptor signaling in nociceptors, but not microglia, abrogates morphine tolerance without disrupting analgesia. *Nat. Med*. **23**, 164–173 (2017).
8. Sun, J., Chen, S.-R., Chen, H. & Pan, H.-L. Opioid receptors in primary sensory neurons are essential for opioid analgesic effect on acute and inflammatory pain and opioid-induced hyperalgesia. *J. Physiol*. **597**, 1661–1675 (2019).
9. Célèrier, E., Laulin, J. P., Corcuff, J. B., Le Moal, M. & Simonnet, G. Progressive enhancement of delayed hyperalgesia induced by repeated heroin administration: a sensitization process. *J. Neurosci. Off. J. Soc. Neurosci*. **21**, 4074–4080 (2001).
10. King, T., Ossipov, M. H., Vanderah, T. W., Porreca, F. & Lai, J. Is paradoxical pain induced by sustained opioid exposure an underlying mechanism of opioid antinociceptive tolerance? *Neurosignals* **14**, 194–205 (2005).
11. Raehal, K. M., Walker, J. K. L. & Bohn, L. M. Morphine side effects in beta-arrestin 2 knockout mice. *J. Pharmacol. Exp. Ther*. **314**, 1195–1201 (2005).
12. Bohn, L. M., Gainetdinov, R. R., Lin, F. T., Lefkowitz, R. J. & Caron, M. G. Mu-opioid receptor desensitization by beta-arrestin-2 determines morphine tolerance but not dependence. *Nature* **408**, 720–723 (2000).
13. Williams, J. T. et al. Regulation of μ-opioid receptors: desensitization, phosphorylation, internalization, and tolerance. *Pharmacol. Rev*. **65**, 223–254 (2013).
14. Adhikary, S. & Williams, J. T. Cellular Tolerance Induced by Chronic Opioids in the Central Nervous System. *Front. Syst. Neurosci*. **16**, 937126 (2022).
15. Yue, X. et al. Sustained morphine treatment augments basal CGRP release from cultured primary sensory neurons in a Raf-1 dependent manner. *Eur. J. Pharmacol*. **584**, 272–277 (2008).
16. Rivat, C. et al. Spinal NK-1 receptor-expressing neurons and descending pathways support fentanyl-induced pain hypersensitivity in a rat model of postoperative pain. *Eur. J. Neurosci*. **29**, 727–737 (2009).
17. Vera-Portocarrero, L. P. et al. Spinal NK-1 receptor expressing neurons mediate opioid-induced hyperalgesia and antinociceptive tolerance via activation of descending pathways. *Pain* **129**, 35–45 (2007).
18. Ma, W., Zheng, W. H., Kar, S. & Quirion, R. Morphine treatment induced calcitonin gene-related peptide and substance P increases in cultured dorsal root ganglion neurons. *Neuroscience* **99**, 529–539 (2000).
19. Drdla, R., Gassner, M., Gingl, E. & Sandkühler, J. Induction of synaptic long-term potentiation after opioid withdrawal. *Science* **325**, 207–210 (2009).
20. Cahill, C. M., Walwyn, W., Taylor, A. M. W., Pradhan, A. A. A. & Evans, C. J. Allostatic Mechanisms of Opioid Tolerance Beyond Desensitization and Downregulation. *Trends Pharmacol. Sci*. **37**, 963–976 (2016).
21. Koshimizu, T.-A. et al. Complex formation between the vasopressin 1b receptor, β-arrestin-2, and the μ-opioid receptor underlies morphine tolerance. *Nat. Neurosci*. **21**, 820–833 (2018).
22. Sharma, S. K., Klee, W. A. & Nirenberg, M. Dual regulation of adenylate cyclase accounts for narcotic dependence and tolerance. *Proc. Natl. Acad. Sci. USA*. **72**, 3092–3096 (1975).
23. Ferrini, F. et al. Morphine hyperalgesia gated through microglia-mediated disruption of neuronal Cl^- homeostasis. *Nat. Neurosci*. **16**, 183–192 (2013).
24. Gardell, L. R. et al. Sustained morphine exposure induces a spinal dynorphin-dependent enhancement of excitatory transmitter release from primary afferent fibers. *J. Neurosci. Off. J. Soc. Neurosci*. **22**, 6747–6755 (2002).
25. Joseph, E. K., Reichling, D. B. & Levine, J. D. Shared mechanisms for opioid tolerance and a transition to chronic pain. *J. Neurosci. Off. J. Soc. Neurosci*. **30**, 4660–4666 (2010).
26. Reichling, D. B. & Levine, J. D. Critical role of nociceptor plasticity in chronic pain. *Trends Neurosci* **32**, 611–618 (2009).
27. Latremoliere, A. & Woolf, C. J. Central sensitization: a generator of pain hypersensitivity by central neural plasticity. *J. Pain Off. J. Am. Pain Soc*. **10**, 895–926 (2009).
28. Mayer, D. J., Mao, J., Holt, J. & Price, D. D. Cellular mechanisms of neuropathic pain, morphine tolerance, and their interactions. *Proc. Natl. Acad. Sci. USA*. **96**, 7731–7736 (1999).
29. Rivat, C. et al. Inhibition of neuronal FLT3 receptor tyrosine kinase alleviates peripheral neuropathic pain in mice. *Nat. Commun*. **9**, 1042 (2018).
30. Araldi, D., Ferrari, L. F. & Levine, J. D. Role of GPCR (mu-opioid)-receptor tyrosine kinase (epidermal growth factor) crosstalk in

opioid-induced hyperalgesic priming (type II). *Pain* **159**, 864–875 (2018).
31. Wang, Y. et al. Blockade of PDGFR-β activation eliminates morphine analgesic tolerance. *Nat. Med.* **18**, 385–387 (2012).
32. Mousa, S. A. et al. Nerve growth factor governs the enhanced ability of opioids to suppress inflammatory pain. *Brain J. Neurol.* **130**, 502–513 (2007).
33. Glass, D. B., Cheng, H. C., Mende-Mueller, L., Reed, J. & Walsh, D. A. Primary structural determinants essential for potent inhibition of cAMP-dependent protein kinase by inhibitory peptides corresponding to the active portion of the heat-stable inhibitor protein. *J. Biol. Chem.* **264**, 8802–8810 (1989).
34. Gao, Y., Nikulina, E., Mellado, W. & Filbin, M. T. Neurotrophins Elevate cAMP to Reach a Threshold Required to Overcome Inhibition by MAG through Extracellular Signal-Regulated Kinase-Dependent Inhibition of Phosphodiesterase. *J. Neurosci.* **23**, 11770–11777 (2003).
35. Crain, S. M. & Shen, K. F. Opioids can evoke direct receptor-mediated excitatory effects on sensory neurons. *Trends Pharmacol. Sci.* **11**, 77–81 (1990).
36. Haller, V. L., Bernstein, M. A. & Welch, S. P. Chronic morphine treatment decreases the Cav1.3 subunit of the L-type calcium channel. *Eur. J. Pharmacol.* **578**, 101–107 (2008).
37. Matus-Leibovitch, N. et al. Chronic morphine administration enhances the expression of Kv1.5 and Kv1.6 voltage-gated K+ channels in rat spinal cord. *Brain Res. Mol. Brain Res.* **40**, 261–270 (1996).
38. Matthes, H. W. et al. Loss of morphine-induced analgesia, reward effect and withdrawal symptoms in mice lacking the mu-opioid-receptor gene. *Nature* **383**, 819–823 (1996).
39. Pogatzki, E. M. & Raja, S. N. A mouse model of incisional pain. *Anesthesiology* **99**, 1023–1027 (2003).
40. Tassou, A. et al. Activation of neuronal FLT3 promotes exaggerated sensorial and emotional pain-related behaviors facilitating the transition from acute to chronic pain. *Prog. Neurobiol.* **222**, 102405 (2023).
41. Gregory, N. S. et al. An overview of animal models of pain: disease models and outcome measures. *J. Pain Off. J. Am. Pain Soc.* **14**, 1255–1269 (2013).
42. Brust, T. F., Conley, J. M. & Watts, V. J. Gα(i/o)-coupled receptor-mediated sensitization of adenylyl cyclase: 40 years later. *Eur. J. Pharmacol.* **763**, 223–232 (2015).
43. Puig, S., Donica, C. L. & Gutstein, H. B. EGFR Signaling Causes Morphine Tolerance and Mechanical Sensitization in Rats. *eNeuro* **7**, ENEURO.0460-18.2020 (2020).
44. Wetzker, R. & Böhmer, F.-D. Transactivation joins multiple tracks to the ERK/MAPK cascade. *Nat. Rev. Mol. Cell Biol.* **4**, 651–657 (2003).
45. Gamble, M. C. et al. Mu-opioid receptor and receptor tyrosine kinase crosstalk: Implications in mechanisms of opioid tolerance, reduced analgesia to neuropathic pain, dependence, and reward. *Front. Syst. Neurosci.* **16**, 1059089 (2022).
46. Volkow, N. D. & Collins, F. S. The Role of Science in the Opioid Crisis. *N. Engl. J. Med.* **377**, 1798 (2017).
47. Safarinejad, M. R. Safety and efficacy of sorafenib in patients with castrate resistant prostate cancer: a Phase II study. *Urol. Oncol.* **28**, 21–27 (2010).
48. Nguyen, M. Q., von Buchholtz, L. J., Reker, A. N., Ryba, N. J. & Davidson, S. Single-nucleus transcriptomic analysis of human dorsal root ganglion neurons. *eLife* **10**, e71752 (2021).
49. Drieu la Rochelle, A. et al. A bifunctional-biased mu-opioid agonist-neuropeptide FF receptor antagonist as analgesic with improved acute and chronic side effects. *Pain* **159**, 1705–1718 (2018).
50. Célèrier, E. et al. Long-lasting hyperalgesia induced by fentanyl in rats: preventive effect of ketamine. *Anesthesiology* **92**, 465–472 (2000).
51. Ventéo, S. et al. Fxyd2 regulates Aδ- and C-fiber mechanosensitivity and is required for the maintenance of neuropathic pain. *Sci. Rep.* **6**, 36407 (2016).
52. Zimmermann, K. et al. Phenotyping sensory nerve endings in vitro in the mouse. *Nat. Protoc.* **4**, 174–196 (2009).
53. Hao, J. et al. The widely used antihistamine mepyramine causes topical pain relief through direct blockade of nociceptor sodium channels. *FASEB J. Off. Publ. Fed. Am. Soc. Exp. Biol.* **35**, e22025 (2021).
54. Torsney, C. & MacDermott, A. B. Disinhibition Opens the Gate to Pathological Pain Signaling in Superficial Neurokinin 1 Receptor-Expressing Neurons in Rat Spinal Cord. *J. Neurosci.* **26**, 1833–1843 (2006).

Acknowledgements

We thank Dr. Lemischka (The Black Family Stem Cell Institute, Icahn School of Medicine at Mount Sinai, New York) for providing the *Flt3* knock-out mice, Dr. Dominique Massotte (UPR3212 Institut des Neurosciences Cellulaires et Intégratives (INCI)) for providing the MOR-mCherry mice. We thank the different technical platforms of Institut des Neurosciences de Montpellier (INM), especially the animal care facility and the functional exploration platform RAM Neuro supervised by Denis Greuet, and RIO imaging platform supervised by Chamroeur Sar. We also thank Dr. Grégory Scherrer for his constructive comments on the manuscript. This work was supported by INM, INSERM, CNRS and Aix-Marseille and Montpellier Universities and grants from: National Research Agency (grant ANR-19-CE16-0008 to C.R.), Fondation pour la Recherche Médicale (DEQ20130326482 to P.D.), CBS2 doctoral school to A.T., A.J., M.T. French ministry of higher education, research and innovation. Biodol Therapeutics, France to J.V. and C.R.

Author contributions

Conceptualization: J.V., C.R.; Methodology: M.A., R.D., P.D., N.F., I.M., J.R., J.V., C.R.; Investigation: C.R., A.T., M.T., M.A., J.R., L.D., A.J., J.P.L., A.G., S.A., F.D., S.M., J.B., CSonrier, CSar, S.V., I.M.; Funding acquisition: R.D., P.D., N.F., D.R., P.S., J.V., C.R.; Project administration: J.V., C.R.; Supervision: J.V., C.R. Writing – original draft: M.A., R.D., P.D., A.T., M.T., J.R., P.C., C.R., P.S., J.V.

Competing interests

C.S., L.D., J.B., and J.P.L. were full-time employees at Biodol Therapeutics. J.V. is inventor of patents (WO2011/083124, WO2016/016370, WO2017211937, EP2023/0779572023) claiming the use of FLT3 inhibitors for the treatment of neuropathic pain and is co-founder of Biodol Therapeutics with P.S. and D.R. The other authors declare no conflict of interests related to the current investigation.

Additional information

Supplementary information The online version contains supplementary material available at https://doi.org/10.1038/s41467-024-54054-y.

Correspondence and requests for materials should be addressed to Jean Valmier or Cyril Rivat.

Peer review information *Nature Communications* thanks the anonymous reviewers for their contribution to the peer review of this work. A peer review file is available.